

The Value of a Cure: An Asset Pricing Perspective*

Viral V. Acharya[†] Timothy Johnson[‡] Suresh Sundaresan[§] Steven Zheng[¶]

September 2021

Abstract

We estimate the value of ending a pandemic using the joint behavior of stock prices and a vaccine progress indicator during 2020. In a general equilibrium model of repeated pandemics, the market response to vaccine progress serves to identify the expected rate of loss of wealth during the pandemic, which, together with the expected time to successful deployment, pins down the economy-wide welfare gain attributable to a cure. With standard preference parameters and using our forecasts during 2020, ending the pandemic would have been worth 5-15% of total wealth. This value rises with greater exposure externality in labor choice. With uncertainty about pandemic frequency and duration, resolving the uncertainty can be as valuable as the cure itself.

JEL Codes: G12, D5, I1, Q54

Keywords : pandemic, vaccine, COVID-19, rare disasters, regime-switching, parameter uncertainty

*First draft: November 15, 2020. We thank Dick Berner, Rob Engle, Stavros Panageas, Matt Richardson, Venky Venkateswaran, and Olivier Wang for their comments and suggestions. We also thank seminar participants at NYU Stern, NYU Stern Quantitative Finance and Econometrics, Advisory Board Meeting of NYU Stern Volatility and Risk Institute, UIUC Gies, IMF, Shanghai Advanced Institute of Finance, UCLA Anderson, and JHU Carey Finance Conference for valuable comments and suggestions. We are grateful to the Vaccine Centre at the London School of Hygiene & Tropical Medicine for sharing publicly available data from their vaccine development tracker. Our vaccine progress indicator (VPI) is available at [ADD URL](#).

[†]Corresponding author. New York University, Stern School of Business, NBER, and CEPR: vacharya@stern.nyu.edu.

[‡]University of Illinois at Urbana-Champaign: tcj@illinois.edu.

[§]Columbia University, Graduate School of Business: ms122@columbia.edu.

[¶]University of California, Berkeley: steven_zheng@berkeley.edu.

1 Introduction

Quantifying the scale of the economic damage caused by a pandemic is a crucial step in assessing policy responses along social, medical, fiscal, and monetary dimensions. This paper builds on the hypothesis that stock markets contained valuable information for gauging the value of ending the coronavirus pandemic during 2020. Stock markets, which corrected by as much as 40-50% at the outbreak of the pandemic in February-March of that year, rebounded robustly within six months. While there are many explanations proposed for the seeming disconnect between the real economy ravaged by the pandemic and the buoyant stock market, one candidate is the progress in development of vaccines.¹ At the time, the arrival (and delivery) of an efficacious vaccine was considered a necessary condition to end the pandemic and lay the foundation for a robust economic recovery.² Stock prices – by reflecting forward-looking expectations – impounded information about the economic value of credible progress in the development of vaccines.

The salience of vaccine development to the stock market is well-illustrated by the following examples. On May 18 and July 14, 2020, *Moderna*, one of the vaccine developing companies, announced good news relating to the progress in its Phase I clinical trials and moving to the next stage of trials. Similarly, on November 9, 2020, *Pfizer* and *BioNTech* announced positive news regarding their Phase III clinical trials. In response to these news, the U.S. stocks gained over \$1 trillion in cumulative market capitalization over these three days, with several pandemic-exposed sectors such as airlines, cruise ships, and hotels experiencing 10-20% appreciations on each day. These moves were both economically large and indicative of time to deployment of a vaccine being an important factor driving variation in stock market prices.³

We build upon these observations and offer an asset pricing perspective to estimate the value of a cure, which we define as the amount of wealth that a representative agent would be willing to pay for obtaining an end to the pandemic. While there are now many estimations in the literature of how costly the pandemic was to the economy, our

¹We use “cure” and “vaccine” interchangeably to denote something that, once deployed, brings the pandemic to an end. Medically, of course, the two mechanisms are distinct.

²See [Lauren Fedor and James Politi, Financial Times, May 18, 2020](#) in the internet appendix.

³See (1) [Matt Levine, Money Stuff, May 19, 2020](#), (2) [Matt Levine, Money Stuff, July 16, 2020](#), (3) [John Authers, Bloomberg Opinion, November 10, 2020](#), and (4) [Laurence Fletcher and Robin Wigglesworth, Financial Times, November 14, 2020](#) in the internet appendix.

approach is different in that it uses stock market data to calculate the *ex ante* value of a cure. Our approach is directly analogous to the seminal work of Lucas (1987) in assessing the welfare costs associated with business cycle risk. Just as that paper provides a framework for assessing the consequences of policy responses to mitigate consumption volatility, our work speaks to the cost-benefit analysis in alleviating the threat of current and future pandemics. Uniquely to the literature studying the welfare cost of disasters, we exploit novel information within the crisis itself to identify the key quantities within our model. Going beyond our baseline estimate for the value of a cure, our work can also shed light on which elements of the economy are driving that value.

Our analysis proceeds as follows.

Our first step is to construct a time series within 2020 of model-based forecasts for the expected time to the widespread deployment of a successful vaccine. Our vaccine progress indicator (VPI) is based on the chronology of stage-by-stage progress of individual vaccine candidates (obtained from the Vaccine Centre at the London School of Hygiene & Tropical Medicine) and related news (obtained from FactSet). Each day, as described in Section 3, we assign probabilities to each active candidate's future transition across developmental phases, or to failure. We then simulate these future transitions for all of the candidates, and each simulation produces a first-to-succeed candidate.⁴ Averaging across simulations gives us that day's forecast for the expected time remaining in the pandemic.

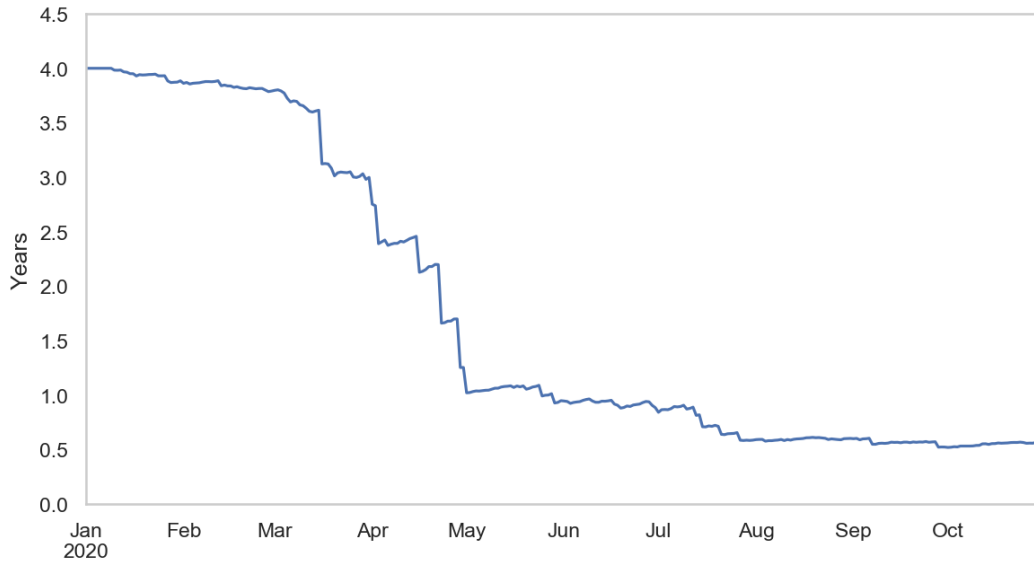
The evolution of our indicator is shown in Figure 1. Note that we do not claim that it is a sufficient statistic for the state of the pandemic at each point in time, nor even for the state of vaccine development. However, it captures one dimension that was watched with intense interest at the time.⁵ Moreover, it turns out to be a key determinant within our exercise of the value of a cure.

We then relate stock market valuations to the expected time to vaccine deployment by regressing returns on changes in our vaccine progress indicator. Controlling for large moves attributable to release of other macroeconomic news, and allowing for some lead-lag structure in the relationship, e.g., due to leakage of news or dating noise in our news

⁴An analogy from credit risk literature is that of a first-to-default basket in which several correlated firms are part of a basket and the quantity of interest is the expected time to a first default.

⁵In Section 3, we compare our forecast to others published during 2020.

Figure 1: Expected Time to Vaccine Deployment



Note: Figure shows our estimate of the expected time to widespread deployment of a COVID-19 vaccine in years.

data, we estimate that a reduction in the expected time to deployment of a vaccine by a year results in an aggregate stock market return of from 4 to 8%. The joint relationship exhibits the anticipated cross-sectional properties, with the co-movement between returns and changes in the vaccine progress indicator being stronger for sectors most affected by the COVID-19 pandemic (see Figure 5). The stock market sensitivity to changes in the VPI is the second crucial empirical quantity that enables us to compute the value of a cure.

Armed with these estimates, we next build and calibrate a general equilibrium regime-switching model of repeated pandemics. We consider an economy with a representative agent who has stochastic differential utility (Epstein-Zin preferences) with endogenous consumption. The state of the economy can be normal, i.e., without a pandemic, or in a pandemic. The nature of a pandemic is that agents are exposed to a health shock that destroys forever a part of the economy's stock of wealth.⁶ Within the pandemic, we model

⁶The permanent loss of capital stock is a common modeling assumption in the rare disaster literature. See (Barro, 2006; Gabaix, 2012; Gourio, 2012; Tsai and Wachter, 2015). In the present case, the loss can be viewed as due to a variety of factors including mortality, attrition of human capital in working from home amidst closures of schools and lack of child care, deadweight losses in asset value due to default, and reallocation frictions in the labor market.

sub-regimes corresponding to the stages of vaccine development. The economy transitions probabilistically across these states. The value of a claim to the economy's output responds to these transitions, and the magnitude of this response identifies the parameters determining the severity and intensity of the pandemic.

Thus, given a value for the expected time to vaccine deployment, the stock market sensitivity that we measure empirically is essentially a sufficient statistic for computing the welfare gain due to escaping the pandemic state, which is our definition of the value of a cure. With standard parameters employed in the literature for preferences and normal time dynamics, the value of a cure turns out to be worth 5-15% of wealth depending on the expected remaining duration of the pandemic, with 5% corresponding to the value in April 2020. This quantity is large relative to *ex post* measures of lost output in 2020.⁷ However, it is consistent with the information in stock market responses to vaccine progress. Moreover, as discussed in Section 4, it is in line with estimates from similar exercises to value the welfare cost of rare disasters.

The paper then extends the model in several directions to explore features that may or may not affect our conclusions.⁸

A first extension endogenizes the real option to invest in vaccine research so that the speed of progress is an equilibrium outcome. Although we do not attempt to estimate a production function for R&D, it is clear *a priori* that the more powerful the available technology the smaller the welfare cost of a pandemic. Nonetheless, we show that given the observed market response to vaccine progress, and the observed expected duration of the pandemic, our calculation of the value of a cure would not be altered under this version of the model.

The next generalization endogenizes the magnitude of health shocks via labor choice in order to study the role of exposure externalities. We assume labor augments agent's capital stock in production; however, it also exposes the agent to the pathogen. The agent thus optimally withdraws labor in the pandemic states, and the magnitude of the labor

⁷While global GDP decreased 3.3% in 2020, the IMF's World Economic Outlook (IMF (2021)) estimates the collapse could have been three times as large had policymakers not enacted significant intervention (including \$16 trillion in fiscal support, for example). They further estimate the cumulative loss in output relative to the counterfactual without COVID-19 to be \$28 trillion over 2020–2025.

⁸To our knowledge, these extensions have not previously been examined in the literature on the welfare cost of disasters or business cycle risk.

withdrawal then determines the equilibrium severity of the shocks to output. However, agents' privately optimal labor choice does not fully internalize the exposure created for other agents.

Using our empirical estimates of the coronavirus severity, and estimates in the literature of the withdrawal of labor in Spring 2020, we compute the difference in the value of a cure with individually optimal labor choice versus that by a central planner. Since the planner imposes a stricter lockdown (or labor contraction) and thus suffers less damage, the value attached to a cure is approximately 15% lower than for the representative agents.⁹ This difference rises with the severity of the externality as measured by the increased degree of lockdown under central planning.

Finally, given the extreme uncertainties during 2020, we relax the assumption that agents in the economy fully understand the (stochastic) properties of the pandemic.¹⁰ Specifically, we assume that agents do not know the regime switching probabilities that govern the expected duration and frequency of pandemics. Using parameter values from the calibration with endogenous labor, we find that the value of the cure rises sharply relative to the full-information model. This effect is stronger – not weaker – when agents have a preference for later resolution of uncertainty (formally, an elasticity of intertemporal substitution that is lower than the inverse coefficient of relative risk aversion). Indeed, we find that the representative agent would be willing to pay as much for resolution of this parameter uncertainty as for the cure itself. An important policy implication is that understanding the fundamental biological and social determinants of future pandemics, may be as important as resolving an immediate pandemic-induced crisis.

To summarize, the contribution of the paper is to bring novel data observed within the 2020 crisis to bear on the important question of the *ex ante* cost of such pandemics. We show that two key quantities that we estimate – the expected duration of the crisis and the stock market response to vaccine progress – are effectively sufficient to identify

⁹We acknowledge, however, that the planner may attach a higher value to the cure if the arrival of the pandemic were to result in social costs outside the capital stock dynamics for the agent.

¹⁰Such uncertainty is natural given the rare nature of pandemics and the evolving understanding of connections between various pandemics (SARS, H1N1, COVID-19, etc.). See, for example, ["COVID-19 Is Bad. But It May Not Be the 'Big One'", Maryn McKenna, Wired, June 17, 2020](#), ["Coronavirus Response Shows the World Is Not Ready for Climate-Induced Pandemics", Jennifer Zhang, Columbia University Earth Institute, February 24, 2020](#), and ["The next pandemic: where is it coming from and how do we stop it?", Leslie Hook, Financial Times, October 29, 2020](#).

the welfare gain to ending the pandemic, which we find to have been 5-15% of wealth in our baseline calibration. This value is robust to endogenizing vaccine investment and labor supply. It rises with the severity of labor externalities and with increased parameter uncertainty.

A couple of clarifications about our exercise are in order. First, the model's depiction of pandemics is a reduced form in the sense that we do not attempt to capture the evolution of an infected population as in standard compartmental (SIR-type) models. This is intentional. The only feature of the coronavirus pandemic that we actually measure empirically is the progress towards a vaccine in 2020 (and the stock market reaction to that progress). Second, we recognize that, in practice, the availability of vaccines in 2021 did not correspond to a "magic bullet" that instantly terminated the spread of COVID-19. However, this does not falsify our analysis.¹¹ The only implicit assumption we are making in mapping vaccine progress to stock market reactions is that, during 2020, investors viewed such progress as informative about when the economy could return to normal.

The rest of the paper is organized as follows. Section 2 relates our work to the existing literature. Section 3 describes the construction of vaccine progress indicator and estimates its covariance with stock market returns during 2020. Section 4 contains our main results: we calibrate a model of recurring pandemics to the empirical evidence and deduce the implied value of a cure. Section 5 presents the extensions described above. Section 6 summarizes and concludes.

2 Related Literature

As noted in the introduction, our approach to quantifying the cost of the pandemic parallels that of Lucas (1987) in assessing the cost of business cycles. While Lucas (1987) finds small welfare improvements to reducing consumption uncertainty, Tallarini Jr (2000) shows that this conclusion is overturned in models with recursive utility when calibrated to match asset pricing moments. Echoing this finding and foreshadowing our own, Barro (2009) reports that, in a model with rare disasters, moderate risk aversion, and an elasticity of intertemporal substitution greater than one, society would willingly pay up to 20% of permanent income to eliminate disaster risk. A number of papers, including Pindyck

¹¹We also note that both our empirical forecasts and our model explicitly allow for uncertainty about the timing and success of an approved vaccine in the post-approval deployment stage.

and Wang (2013), explore the welfare costs associated with climate risk. The latter work addresses the issue of how much should society be willing to pay to reduce the probability or impact of a catastrophe.

A different approach to determining agent's valuation of alternative consumption paths is presented by Alvarez and Jermann (2004) who define the "marginal cost" of business cycles as the ratio of a market price of a claim to the true consumption process to that of an alternative path with the same mean but lower uncertainty. While this approach has the advantage of being preference-free, it is not obvious how to attain the required market prices. (It may well be applicable in the future if pandemic insurance becomes widely traded.)

Our model is related to Ai (2010) and Gourio (2012). We share many of features of each, but differ by offering a setting that allows us to connect to our unique empirical data. Both of those papers feature shocks to the stock of productive capital, with endogenous consumption. Like Ai (2010), our model is in continuous time and allows for frictionless adjustment to capital. That paper also studies the effect of parameter uncertainty, although not in a setting with rare disasters. We differ from Gourio (2012) in modelling *extended* disasters, like pandemics, whose *expected duration* is a crucial and evolving feature of the economy.

While the literature studying the economic impact of COVID-19 has exploded in a short period of time, there is relatively little focus on the role played by vaccine development and its progress. We first relate to the theoretical literature in asset pricing that is closest to our model; we then relate to the empirical literature on observed contraction in employment and consumption during the pandemic.

Hong et al. (2020b) study the effect of pandemics on firm valuation by embedding an asset pricing framework with disease dynamics and a stochastic transmission rate, equipping firms with pandemic mitigation technologies. Similar to our paper, they model vaccine arrival as a Poisson jump process between pandemic and non-pandemic states. Hong et al. (2020a) combine the model of Hong et al. (2020b) with pre- and post-COVID-19 analyst forecasts to infer market expectations regarding the arrival rate of an effective vaccine and to estimate the direct effect of infections on growth rates of earnings. In particular, they develop a regime-switching model of sector-level earnings with shifts in their first and second moments across regimes.

In both of these papers, the pricing kernel is exogenously specified for the pandemic and the non-pandemic states. In contrast, our model is general equilibrium in nature with the representative agent optimally choosing labor and consumption (and, in turn, investment in capital) to mitigate health risk. Deriving asset prices from first principles in a regime-switching framework of pandemics – which allows for several sub-states in a pandemic relating to vaccine progress – is an important theoretical contribution of our paper. We build upon this setup further to introduce learning when there is parameter uncertainty about pandemic parameters.¹²

For empirical work, Hong et al. (2020b) fix expected pandemic duration around one year but show in comparative statics that asset prices show considerable sensitivity to the arrival rate of the vaccine. Hong et al. (2020a) use their model to infer the arrival rate of the vaccine. In contrast, we provide a “vaccine progress indicator” in the form of an estimated time to vaccine deployment using actual data and related news on the progress of clinical trials of vaccines for COVID-19. We relate this vaccine progress indicator to stock market returns to infer the loss in economic wealth in the pandemic state relative to the non-pandemic state.

Elenev et al. (2020) incorporate a pandemic state with low, disperse firm productivity that recurs with low probability for studying government intervention in corporate credit markets. While we do not model credit markets in our setup, our differentiating novel features are: construction of a vaccine progress indicator and estimation of its joint relationship with stock markets, and mapping it into a general equilibrium regime-switching model of pandemics with asset prices in order to derive an estimate of the value of a cure.

Kozlowski et al. (2020) model learning effects that lead to long-term scarring after the pandemic is over as policy responses relating to debt forgiveness in the current pandemic can lead to lower leverage and consumption post-pandemic. Through the learning channel in our model, there can also be “scarring” effects wherein agent’s consumption upon exit from a pandemic does not revert to the pre-pandemic levels due to the increase in updated probability of future pandemics. This, however, is not the focus of our paper.

Collin-Dufresne et al. (2016) show that learning can amplify the pricing of macroe-

¹²On a technical front, Hong et al. (2020b,a) consider aggregate transmission risk into SIR-style model, whereas our model of health risk arising from a pandemic is closer to the literature on rare disasters cited in the Introduction.

conomic shocks when the representative agent has Epstein-Zin preferences and Bayesian updating. Our results on learning and the impact of parameter uncertainty on the value of a cure are related to the findings of both these papers; our model can generate both long-term scarring in consumption due to updated probability of pandemics and significant contraction of labor and consumption when parameter uncertainty is high, when the elasticity of intertemporal substitution (EIS) is low. Interestingly, expected time to deployment of a vaccine can be considered as a “macroeconomic shock” in our model that affects asset prices and depends crucially on parameter uncertainty in a manner that interacts with deep preference parameters.

3 Vaccine Progress Indicator and its Covariance with Stock Returns

As described in the introduction, the paper’s hypothesis is that the stock market may convey important information about the social value of resolving the pandemic. This section explains how we attempt to extract that information. There are two distinct steps. First, we construct a method for summarizing the state of vaccine research throughout 2020. Second, we estimate the stock market response to its changes.

3.1 Measuring Vaccine Progress

Readers are, by now, broadly familiar with the contours of the global effort to develop a vaccine for COVID-19 during 2020. Through many of the excellent tracker apps, dashboards, and periodic survey articles we were all educated about the dozens of candidates under study, and their progress through pre-clinical work and clinical trials. On any given day, the state of the entire enterprise was a high-dimensional object consisting of multiple pieces of information about all of the projects. Our goal is to reduce that high dimensional object to a single number. Also, crucially, the number should have a tangible physical (or biological or economic) interpretation.

The single most salient aspect of vaccine development, the number that nearly all discussions boiled down to, was the anticipated time until widespread availability of a proven candidate (“when will it end?”). We therefore construct an estimator of that quantity using a stochastic model of vaccine progress with three main ingredients to match the

real-world development of COVID-19 vaccines.

First, the model simulates the full stage-by-stage progress of each candidate in “real-time” in order to estimate the time until the first candidate successfully deploys. Specifically, each run of the simulation takes the current stage of each candidate, then simulates forward the entire clinical timeline through pre-clinical trials, clinical trials, application submission, regulatory approval and vaccine deployment.¹³ Each stage is characterized by a duration and a probability of failing or advancing onto the next stage. At each simulated stage, each candidate can either fail (and that candidate’s run ends) or advance onto the next stage (and the simulation continues). The model then records the time to deployment among candidates successfully reaching deployment, and the average time across a large number of runs is that day’s estimate of the expected time until vaccine deployment. Finally, the model advances to the next day and repeats the simulation for the next day’s estimate.

We model vaccine deployment as a final stage with a non-zero probability of failure rather than an absorbing state after regulatory approval. That is, an approved vaccine possibly still could not attain widespread deployment, e.g., due to manufacturing and distribution difficulty, emergence of serious safety concerns, mutation of the virus, or adoption hesitancy. In other words, the approval of a vaccine without full deployment does not correspond to a “magic bullet” that instantly terminates the spread of COVID-19 and ends the pandemic.

Second, vaccine candidates exhibited notable correlation in their development and expected outcomes. This positive dependence among candidates arises most obviously because all candidates are targeting the same pathogen, and will succeed or fail largely due to its inherent biological strengths and weaknesses. Candidates also share one of a handful of strategies (or platforms) for stimulating immunological response,¹⁴ rely on common technological components, resources or abilities, and some research teams concurrently

¹³This is a simplification. Candidate vaccines will actually undergo multiple overlapping trial sequences with different patient populations, delivery modalities, or medical objectives (endpoints). One sequence could fail while others succeed. Trials can also combine phases I and II or II and III. In our empirical implementation we focus on the most advanced trial of a candidate. This follows Wong et al. (2018).

¹⁴For example, if an RNA-based platform proves to be safe and effective, then all candidates in this family would have a higher likelihood of success. In October 2020, two candidate vaccines had their trials paused due to adverse reactions: both were based on adenovirus platforms.

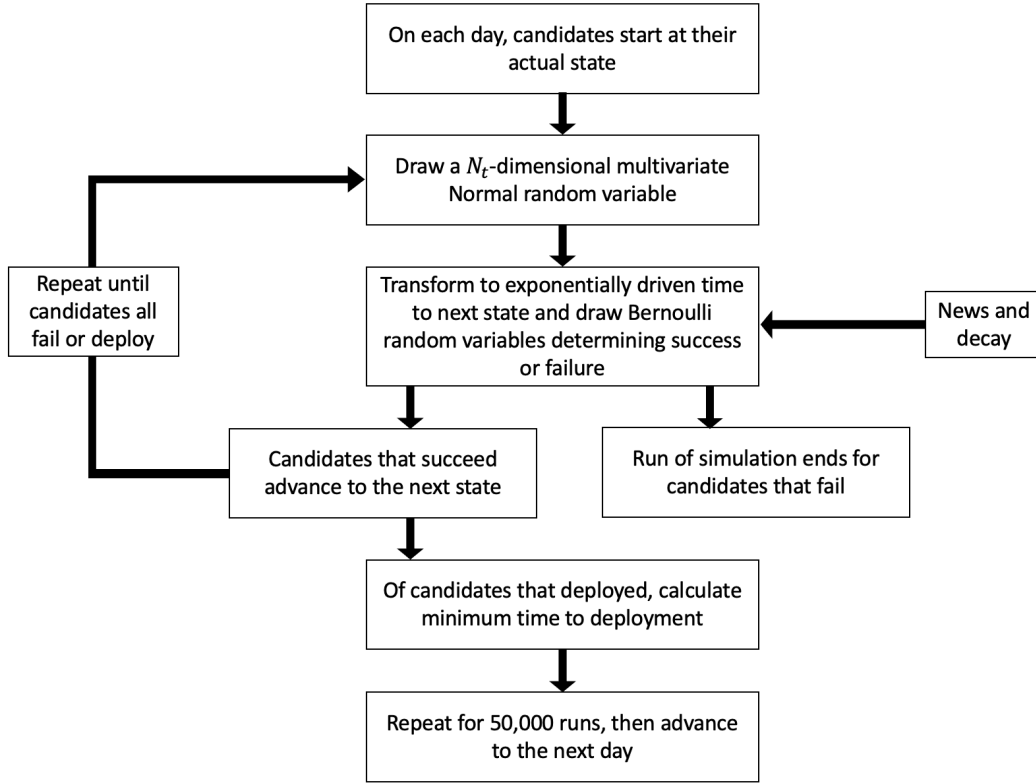
develop several candidate vaccines.¹⁵ The model incorporates correlation among candidates by assuming the stochastic duration of each stage (across candidates) are generated by a Gaussian copula with positive correlation matrix.

Third, as described so far, the “state” of each candidate is simply its current clinical trial state. However, this not realistic for two reasons. First, the initiation of a new state is often announced in advance, so the actual advancement into the next state is already known ahead of time. Second, the “state” is not static in the sense that there is still progress within a clinical trial. Preliminary results or more complete information about earlier trials may be published, released to the press, or leaked. Trial schedule information (delays or accelerated timelines) may be announced. And regulatory actions by non-U.S. authorities may also convey relevant information. To incorporate the real-time announcement of information pertinent to vaccine progress, the model adjusts the probability of each candidate’s current-stage success on the date of arrival of news specific to it. Because positive news is more likely to be revealed than negative news, the model also deterministically depreciates each candidate’s success probability in the absence of news. We will verify below that our conclusions about the stock market response to vaccine progress are not driven by assumptions regarding the arrival of interim trial news.¹⁶

Figure 1 shows the model’s estimation of the expected time to widespread deployment from January through October of 2020. The index is almost monotonically declining, since there were no reported trial failures and very few instances of negative news through at least August. The crucial aspects of the index for our purposes are the timing and sizes of the down jumps corresponding to the arrival of good news.

The next subsection provides details on the data and the mathematical construction of the forecast time-series, and discusses some of the underlying assumptions.

Figure 2: Simulation Flow Chart



Note: Figure shows the simulation that estimates the expected time until vaccine deployment.

3.1.1 Forecast Construction

Figure 2 outlines the simulation procedure. We start with N positively correlated vaccine candidates, with correlation matrix \mathcal{R} . Each candidate n is in a state $s \in S$, where

$$S = \{\text{failure, preclinical, phase 1, phase 2, phase 3, application, approval, deployment}\}$$

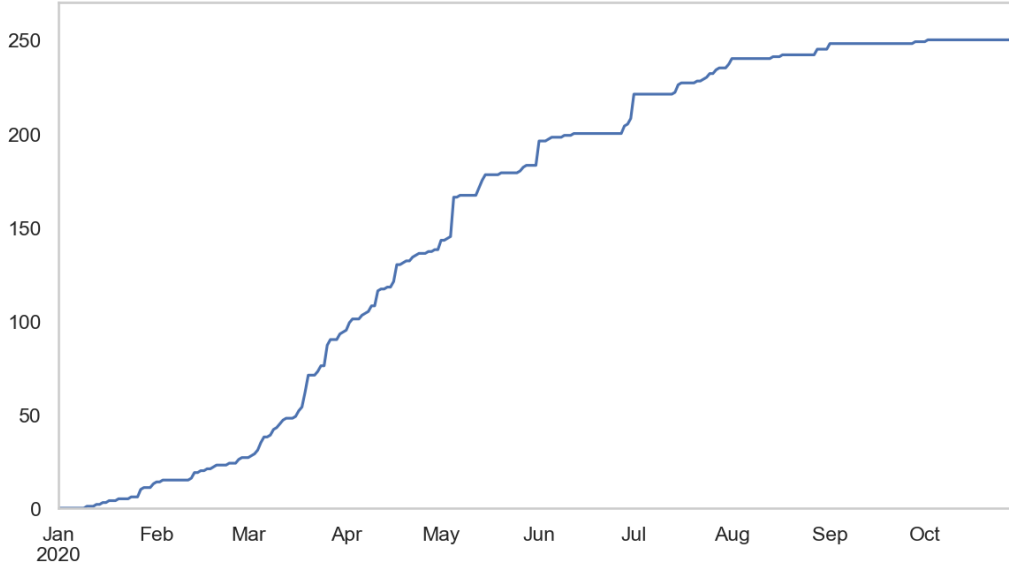
and each state has known expected duration τ_s and baseline probability of success Π_s^{base} .

Next we augment the state-level, baseline probability of successes with candidate-

¹⁵Negative correlation could also potentially arise if the approval of one candidate caused regulators to raise the bar for efficacy of remaining candidates, or caused resources to be diverted away from competing projects.

¹⁶Technically, altering the marginal success probabilities within a trial induces a non-exponential unconditional marginal distribution of trial duration. We retain the exponential assumption of the Gaussian copula for tractability. Our results are robust to using constant probabilities.

Figure 3: Number of Active COVID-19 Vaccine Projects



Note: Figure shows the number of active COVID-19 vaccine candidates. Data as of November 2020.

specific news. Let $\omega_{n,t} \in \Omega$ denote news published at time t about candidate n . For example, Ω could span positive data releases, negative data releases, next state announcements, etc. Then let $\Delta\pi : \rightarrow [-1, 1]$ be a mapping from news to changes in probabilities. For each candidate, we cumulate the changes in probabilities from all news from the beginning of our sample t_0 up to time t ,

$$\Delta\pi_{n,t}^{\text{news}} = \sum_{t'=t_0}^t \Delta\pi(\omega_{n,t'}).$$

Finally, we combine it with the baseline probability of success, resulting in a candidate-specific probability of success that potentially varies over time, even within the same state,

$$\pi_{n,s,t}^{\text{total}} = \frac{\exp Y_{n,s,t}}{1 + \exp Y_{n,s,t}}$$

where $Y_{n,s,t} = \log \frac{\pi_s^{\text{base}}}{1 - \pi_s^{\text{base}}} + 2\Delta\pi_{n,t}^{\text{news}}$.

We simulate stage-by-stage progress of each candidate and generate the expected time

to first vaccine deployment, similar to a first to “default” model. Specifically, on each day, one run of the simulation repeats steps one and two until candidates have all failed or deployed:

1. We model each state transition as a 2-state Markov chain with exponentially distributed times. Draw an N -dimensional multivariate normal random variable

$$z_t = [z_{1,t}, \dots, z_{N,t}]' \sim \mathcal{N}(0, \mathcal{R})$$

and for each candidate, transform to exponential time with intensity $\lambda_{n,s,t} = \frac{\pi_{n,s,t}}{\tau_s}$

$$t_{n,s,t} = -\frac{\log \Phi(z_{n,t})}{\lambda_{n,s,t}}.$$

2. Then draw a success or failure Bernoulli random variable with parameter π_s . If failure, then that candidate’s run is over. Else if success, then that candidate advances states and the run continues.
3. Calculate each candidate’s time to vaccine deployment as

$$T_n = \begin{cases} \sum_s t_{n,s,t} & , \text{ if candidate deploys} \\ \infty & , \text{ if candidate fails} \end{cases}$$

4. Then calculate minimum time to vaccine deployment across candidates, $\min_n T_n$.

That finishes one run of the simulation. We repeat for 50,000 runs and take the cross-run average as T^D , before advancing to the next day. On each day across runs, we calculate the average

$$\mathbb{E}[T^*] = (1 - \mu)T_t^D + \mu T^{ND},$$

where some fraction, μ , of simulations will result in all candidates not reaching deployment, so we incorporate T^{ND} , an estimated expected time to deployment by a project outside of our sample.¹⁷ In addition to the mean, the model also delivers the full distri-

¹⁷The model does not attempt to forecast the entry of new projects.

bution, and hence all quantiles, of the expected time until vaccine deployment as of each date.

We obtain the pre-clinical dates and trial history of vaccine candidates from publicly available data collated by the London School of Hygiene & Tropical Medicine (LSHTM). We observe the start dates and durations of each pre-clinical and clinical trial, along with their vaccine strategy.¹⁸ We augment the LSHTM timeline with news pertinent to vaccine progress from FactSet StreetAccount.¹⁹ The model necessarily involves many parameters for which we have little hope of obtaining precise estimates. Details of our choices of all parameters are explained in the Internet Appendix. We will validate our choices both by examining robustness to reasonable variations and by comparing them to other actual *ex ante* forecasts published during the sample period.²⁰

Our indicator of vaccine progress aims to capture expectations about deployment principally in the U.S. since this is likely to be the primary concern of U.S. markets. Because of political considerations, we believe that observers at the time judged it to be very improbable that vaccines being developed in China and Russia would be the first to achieve widespread deployment in the U.S. Our base case construction for this reason omits candidates coded in the LSHTM data as originating in these countries.²¹ This assumption is consistent with the progress of these candidates receiving minimal coverage in the U.S. financial press. We will also verify that including them in our index does not change our primary results.

It is worth acknowledging that, in focusing on the scientific advancement of the individual candidates, our measure does not attempt to capture general news about the vaccine development environment and policy. For example, news about the acquisition and deployment of delivery infrastructure by governments (or the failure to do so) could certainly affect estimates of the time to availability. We also do not capture the news content of government financial support programs or pre-purchase agreements. The Fall of 2020 saw open debate about the standards that would be applied for regulatory approval, the

¹⁸The Internet Appendix includes more detail on the number of candidates and breakdown of strategies.

¹⁹We classify vaccine related stories into seven positive types and six negative types. The types and probability adjustments are given in the Internet appendix.

²⁰The appendix also presents evidence that our distributional assumptions are reasonably consistent with the (small) set of observed trial outcomes.

²¹We retain candidates coded as multi-country projects including Russia or China.

outcome of which could have affected forecasts as well. While we could alter our index based on some subjective assessment of the impact of news of this type, we feel we have less basis for making such adjustments than we do for modeling clinical trial progress.

Figure 1 shows the model’s estimation of the expected time to widespread deployment from January through October of 2020, and Figure 3 shows the number of active vaccine projects. The starting value of the index, in January, is determined by our choice of the parameter T^{ND} because, with very few candidates and none in clinical trials, there was a high probability that the first success would come from a candidate not yet active. However this parameter effectively becomes irrelevant by March when there are dozens of projects.

3.1.2 Validation

We are aware of two datasets that contain actual forecasts of vaccine arrival times, as made in real-time. As a validation check, we compare our index to these.

The two data sets are surveys, to which individuals supplied their forecasts of the earliest date of vaccine availability. Comparisons between these pooled forecasts and our index require some intermediate steps and assumptions. In both cases, the outcomes being forecast are given as pre-specified date ranges. Thus, on each survey date, we know the percentage of respondents whose point forecast fell in each bin. For each survey we estimate the median response, assuming a uniform distribution of responses within the bin containing the median.²² Under the same assumption, we can also tabulate the percentage of forecasters above and below our index.

The first survey is conducted by Deutsche Bank and sent to 800 “global market participants” asking them when they think the first “working” vaccine will be “available”. The survey was conducted four times between May and September. The second survey is conducted by Good Judgement Inc., a consulting firm that solicits the opinion of “elite super-forecasters.” Their question asks specifically “when will enough doses of FDA-approved COVID-19 vaccine(s) to inoculate 25 million people be distributed in the United States?”

²²While it is tempting to equate the surveys’ distribution of forecasts with a forecasted distribution, these are conceptually distinct objects that need not coincide. In addition, in each survey, the farthest out forecast bin is unbounded, meaning that “never” (or “more than 3 years from now”) is a possible response. So, for both reasons, it is problematic to compute a weighted average forecast across the response bins. The modal response bin is also not a good summary statistic for the same reason, and also because it depends on the bin widths.

(Information about the number of responders is not available.) Responses are tabulated daily, starting from April 24th. For brevity, we examine month-end dates. Table 1 summarizes the comparison.

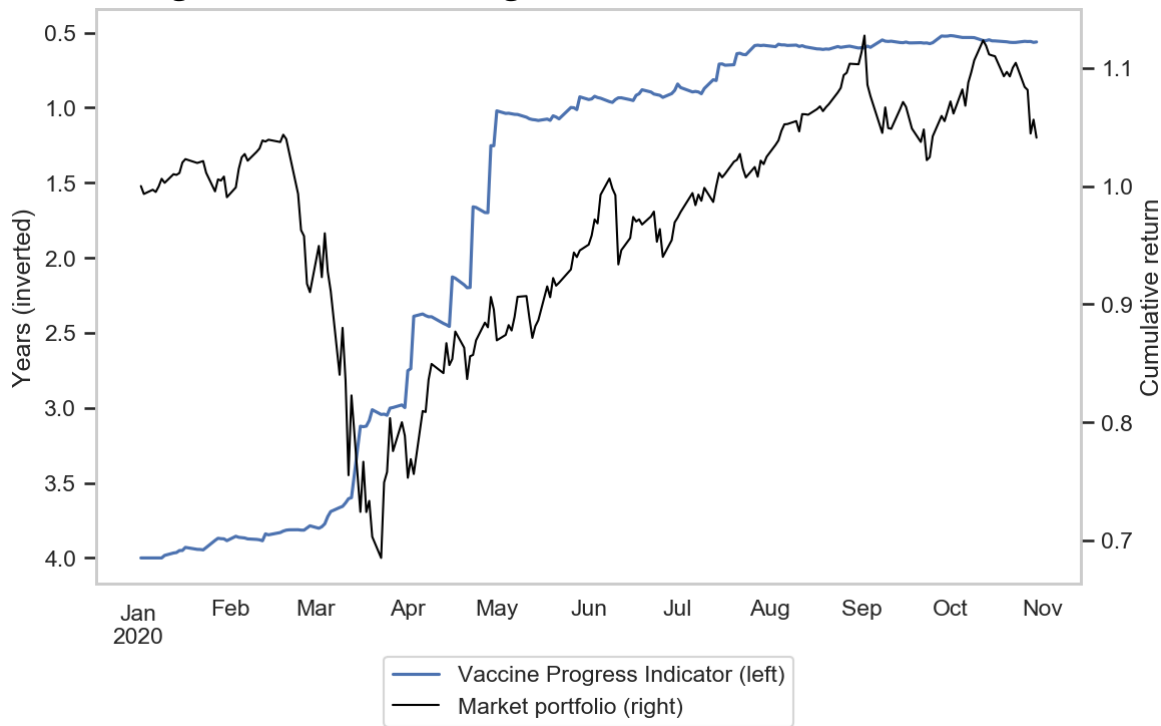
Our forecasts align well with those of the Deutsche Bank survey, though ours are more optimistic than the median. The optimism is more pronounced when compared to the superforecasters early in the pandemic. Although we are within the interquartile range of forecasts after May, the earlier dates see us in the left-tail of the distribution. A possible reason is the specificity of the particular survey question, which specifies an exact quantity of the vaccine being distributed in the United States. Respondents may have more skepticism of feasible deployment than we have assumed. We will examine robustness of our results below to increasing the probability of an approved vaccine failing in the deployment stage.

3.2 Stock Market Response

Figure 4 plots vaccine progress (inverted) along with the market portfolio's year-to-date performance. In principle, assessing the stock market response to changes in vaccine progress should be straightforward. However, the circumstances of 2020 complicate the task. In a nutshell, there was a lot else (such as fiscal and monetary policy actions, government risk-sharing of vaccine development, etc.) going on. The amount of information for markets to digest was enormous and multifaceted. Even the information flow just about coronavirus research *other than vaccine trials* was voluminous. Thus, how to control for non-vaccine related news becomes an important consideration.

Our approach is to run daily regressions of stock market returns on vaccine progress and exclude days with large stock market moves that were reliably judged to be due to other sources of news. Specifically, we employ the classification of Baker et al. (2020b) for causes of market moves greater than 2.5% in absolute value. Those authors enlist the opinion of three analysts for each such day and ask them to assign weights to *types* of causes (e.g., corporate news, election results, monetary policy, etc). Under their classification, research on vaccines falls under their "other" category, whereas news about the pandemic itself was usually categorized as "macroeconomic". We view market returns on such days as very unlikely to have been driven by vaccine news if none of the three analysts assigns more than 25% weight to the other category, or if the return was more

Figure 4: Vaccine Progress and Market Performance



Note: Figure plots vaccine progress (inverted and left axis) along with the cumulated year-to-date excess return on the value-weight CRSP index (right axis). The risk-free rate is the one-month Treasury bill rate.

negative than -2.5%. The latter exclusion is based on the fact that there were no significant vaccine setbacks prior to the end of our data window,²³ and on the prior knowledge that positive vaccine progress cannot be negative news. We include dummies for all of the non-vaccine large-news days. There are 28 such days, 17 of which were in March.

Our approach is imperfect. We have no other controls outside these large move days when there were certainly other factors influencing markets. Including dummy variables effectively reduces our sample size. However, at a minimum we are limiting the ability of our estimation to misattribute the largest market moves to vaccine progress.

Table 2 shows the resulting regression estimates of market impact. These regression specifications include changes in the vaccine progress indicator in a five day window

²³As of the time of this draft, Baker et al. (2020b)'s website had classified days through June. We append September 3 and September 23 as two dates with negative jumps but arguably were driven by non-vaccine progress related news.

around each day, t , on which stock returns are measured. Including changes on days other than the event day- t guards against our imperfect attribution of the date of news arrival. *A priori* we suspect it is more likely that, if anything, markets have information before it is reflected in our index, meaning the relevant reaction would correspond to the $t + 1$ or $t + 2$ coefficients. On the other hand, given the sheer volume of news being processed during this period, we do not rule out delayed incorporation of information, which would show up in the $t - 1$ or $t - 2$ coefficients. The specifications also include two lags of the dependent variable to control for short-term liquidity effects. Specifically, the regression is

$$R_{m,t}^e = \alpha + \sum_{h=-2}^2 \beta_h \Delta \text{VPI}_{t+h} + \gamma_1 R_{m,t-1}^e + \gamma_2 R_{m,t-2}^e + \sum_{j=1}^{28} \delta_j \mathbb{1}_{\text{jump } j} + \epsilon_t \quad (1)$$

where ΔVPI_t is the change in vaccine progress indicator, and $\mathbb{1}_{\text{jump } j}$ is a dummy equal to one on the j th jump date from Baker et al. (2020b). The dependent variable is the return to the value-weighted CRSP index from January 1 through October 31, 2020.

The first column of the table shows results using our baseline vaccine progress indicator. The coefficient pattern shows the largest negative responses on the $t - 1$ and $t + 2$ index changes. Focusing on the cumulative impact, the sum of the β s is statistically significant at the 1% level. The precisely estimated point estimate implies a stock market increase of 8.6 percent on a decrease in expected time to deployment of one year. This number seems plausible: subsequent to our sample, on November 9th the U.S. stock market opened almost 4% higher in response to positive news from Pfizer on Phase III trial results. This would imply more sensitivity than the OLS estimate if, as seems likely, the news revised estimates of time to deployment by less than six months.²⁴

Returning to Table 2, the second and third columns implement the methodology of Kogan et al. (2017) (hereafter KPSS). Those authors use an empirical Bayes procedure to estimate the market value of patents using the stock returns to the patenting firm in an

²⁴While it is not the focus of the paper, it is also interesting to ask about the total contribution of vaccine progress to the stock market performance during the sample period, and to the post-March rally in particular. From March 23 to October 30 our forecast dropped by 2.5 years, of which 0.6 years was expected. The OLS point estimate then implies that vaccine news in total would have induced a 16.3% positive return. The return on the S&P 500 during this period was 47.7%. Hence, vaccine progress could have been responsible for 34% (16.3/47.7-1) of the rally.

event window surrounding patent publication date. As in our case, economic logic rules out a negative response: vaccine progress cannot be unfavorable news just as the value of a patent must be positive. KPSS employ a truncated normal prior distribution for the unobserved true response. Conditional on knowing the return standard deviation, the posterior mean estimate of the response coefficient is then also distributed as a truncated normal. The estimation methodology generalizes naturally to a multivariate regression setting²⁵ (O’hagan (1973)). The table reports posterior mean and standard deviations for the individual response coefficients and for their sum.²⁶ The methodology is sensitive to the specification of the prior variance of the coefficient distribution. Both column 2 and column 3 assume that the pre-truncated normal distribution for β_t has standard deviation equal to 1, which, after truncation, implies that 84% of the distribution mass is below 1.0. We regard this as a conservative (or skeptical) choice.²⁷ Results in the second column use the same (independent) prior for all the response coefficients. The third column uses a smaller prior mean for the lead and lag coefficients.²⁸ Both priors produce posterior means for the sum of the five response coefficients that are lower than the OLS estimate: -6.4% in column 2 and -4.1% in column 3. Note that the estimation is sharp in both cases in the sense that each posterior mean is several standard deviations from zero. The calibrations in the next section will adopt the range of these conservative estimates.

To examine the robustness of the response estimates to the assumptions built into the vaccine progress index, we repeat the OLS specification estimation with five variants. These results are shown in Table 3. The first column repeats the original specification from the prior table. The next two columns vary the assumptions about the effect of news to phase success probabilities. (Column 2 includes no news adjustments. Column 3 applies the news adjustments to only the current trial phase, as opposed to all future phases, and

²⁵We follow KPSS in assuming a zero mean under the prior for the pre-truncated normal distribution, assuming returns are normally distributed, and in using the regression residual to estimate the return standard deviation. Note that the estimation still includes dummy variable for market jump days making the normality assumption plausible.

²⁶Moments of the truncated multivariate normal posterior are computed using the algorithm of Kan and Robotti (2017) using software provided by Raymond Kan. <http://www-2.rotman.utoronto.ca/~kan/research.htm>.

²⁷Note that making the prior more diffuse does not, in this case, correspond to making it less informative: the prior mean increases with the standard deviation.

²⁸Specifically, the assumption is that pre-truncated standard deviations are 0.7 for the first lead and lag and 0.5 for the second lead and lag.

increases the $\Delta\pi$ from news on positive data releases, positive enrollment and dose starts to 15%, 5% and 5%, respectively) The fourth column increases the base copula correlation from 0.2 to 0.4. The fifth column lowers the assumed probability of successful deployment following regulatory approval. As mentioned above, a lower probability of successful deployment may accommodate real-life set backs such as distribution difficulty, emergence of safety concerns, mutations of the virus, or adoption hesitancy. Finally the sixth column includes vaccine candidates whose research program is based in Russia or China. In all of these cases the sum of the response coefficients is highly statistically significant and the point estimates are in the same range as those in Table 2.²⁹

3.3 Industry Responses

As a validity check for our primary findings, we examine the price impact of vaccine progress in the cross-section of industries. We first gauge each industry's exposure to COVID-19 by its cumulative return from February 1, 2020 to March 22, 2020. This period captures the rapid onset of COVID-19 in the US, with a public health emergency being declared on January 31, 2020³⁰ and a national emergency declared on March 13, 2020.³¹ Importantly, this period precedes the Federal Reserve's announcement of the Primary Market Corporate Credit Facility and Secondary Market Corporate Credit Facility on March 23, 2020³² and significant advances in vaccine progress, helping us pin down industry covariances with COVID-19 itself, separate from covariances with monetary policy responses and vaccine progress.

We then estimate industry sensitivity to vaccine progress over the non-overlapping sample from March 23, 2020 to October 31, 2020, by re-estimating (1) sector-by-sector,

$$R_{i,t}^e = \alpha + \sum_{h=-2}^2 \beta_{h,i} \Delta VPI_{t+h} + \gamma_{1,i} R_{i,t-1}^e + \gamma_2 R_{i,t-2}^e + \sum_{j=1}^{28} \delta_{j,i} \mathbb{1}_{\text{jump } j} + \epsilon_{i,t} \quad (2)$$

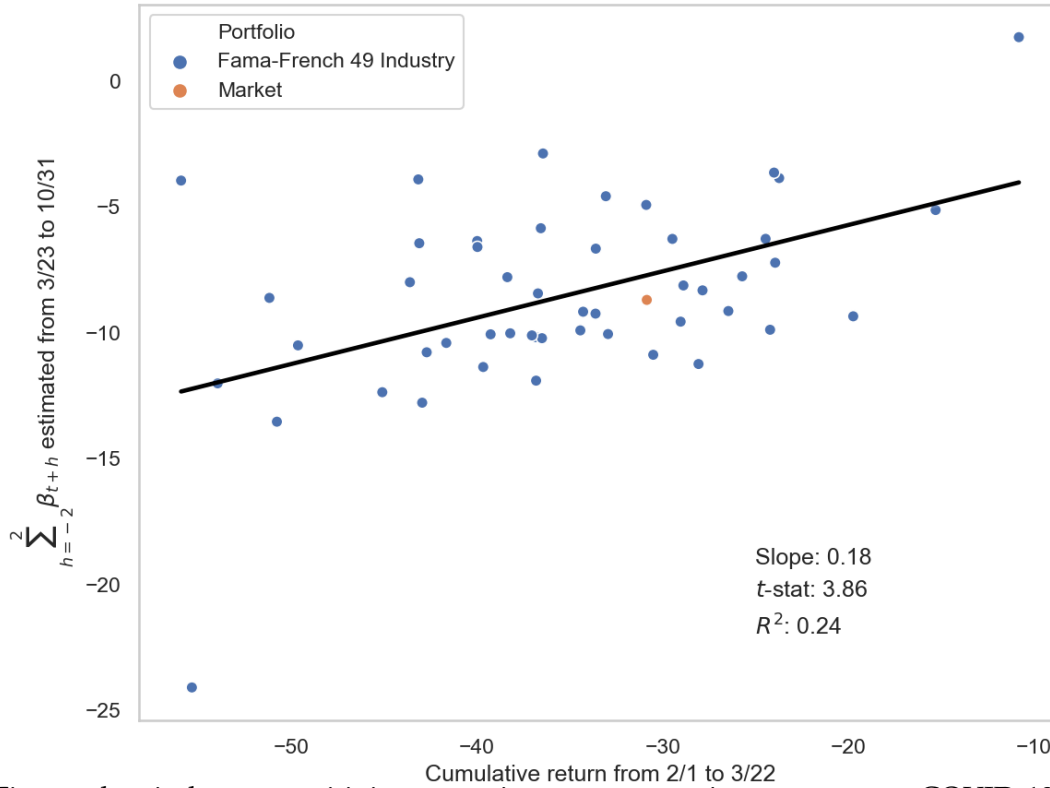
²⁹We further explore adjusting each candidate's state-level duration, in addition to probability of success, using relevant news. Our findings are robust to these additional specifications. Results are available upon request.

³⁰<https://www.hhs.gov/about/news/2020/01/31/secretary-azar-declares-public-health-emergency-us-2019-novel-coronavirus.html>

³¹<https://www.whitehouse.gov/presidential-actions/proclamation-declaring-national-emergency-concerning-novel-coronavirus-disease-covid-19-outbreak/>

³²<https://www.federalreserve.gov/monetarypolicy/pmccf.htm>

Figure 5: Industry Sensitivity to Vaccine Progress



Note: Figure plots industry sensitivity to vaccine progress against exposure to COVID-19 as measured by cumulative returns. Cumulative returns are from February 1, 2020 to March 22, 2020. Sensitivity to vaccine progress is estimated from March 23, 2020 to October 31, 2020 as in (2).

where $R_{i,t}^e$ is value-weight excess returns on the 49 Fama-French industry portfolios.

Figure 5 presents the results. Each industry’s sensitivity to vaccine progress is plotted against its exposure to COVID-19. The relationship is negative and statistically significant – industries that were more exposed to COVID-19 subsequently saw more positive price impact as the vaccine was expected to deploy sooner. The industries also exhibit notable variation. Oil, fabricated products and recreation were among those with higher COVID-19 exposure and vaccine progress sensitivity, while pharmaceutical products, food products and computer software had lower exposure and sensitivity. The association of industry exposure to COVID-19 with its subsequent sensitivity to our index lends confidence to the construction and interpretation of the index as, in fact, measuring vaccine progress. Hence, the results here make it unlikely that our primary findings on the market’s sensi-

tivity are due to omitted variables.³³

4 Markov State Model of Pandemics

In this section, we introduce a regime-switching model of pandemics in order to derive the value of a cure in terms of the economy's primitive objects. In order to connect the theory to our empirical exercise, we need a model with four attributes: a description of pandemics; a well-defined notion of the value of ending a pandemic; a depiction of progress towards that objective; and a stock market that is sensitive to that progress. Our fundamental view of a pandemic is as a process that destroys household wealth, as in Gourio (2012), with consumption and other policies potentially responding endogenously. For this reason, we work with a production-based framework rather than an endowment economy.

4.1 Pandemic Dynamics

We consider the state of the economy to be either in "non-pandemic" regime or in "pandemic" regime. Within the pandemic regime, there can be several sub-states that correspond in our context to different stages in the development of vaccines. We denote the state as $s \in \{0, 1, \dots, S - 1, S\}$, where for ease of notation both state 0 and state S are the same non-pandemic states, and the others are pandemic states. We assume that the economy switches between these states based on a Markov-switching or transition matrix.

³³One omitted variable of interest might be monetary policy. In our time-series framework, we looked directly at stock returns while controlling for large market-moving events attributable to monetary policy (among other news unrelated to vaccine progress) using dates from Baker et al. (2020b). Evidence in Hong et al. (2020a) and Gormsen and Kojen (2020), respectively, supports a revision in corporate cash flows during the pandemic, by examining expectations of stocks' earnings and implied dividend yields, i.e., an improvement in the numerator of a stock's valuation formula as distinct from the (discount) interest rate in the denominator. Our cross-sectional tests also provide robustness to the interpretation that market's sensitivity to vaccine progress is driven by such progress improving the economic prospects of pandemic-affected sectors.

The transition probabilities are given as follows:

$$Pr(s_{t+dt} = 1 | s_t = 0 \text{ or } S) = \eta dt \quad (3)$$

$$Pr(s_{t+dt} = s_t | s_t = 0 \text{ or } S) = 1 - \eta dt \quad (4)$$

$$Pr(s_{t+dt} = s - 1 | s_t = s \in [1, S - 1]) = \lambda_d(s) dt \quad (5)$$

$$Pr(s_{t+dt} = s + 1 | s_t = s \in [1, S - 1]) = \lambda_u(s) dt \quad (6)$$

$$Pr(s_{t+dt} = s_t | s_t = s \in [1, S - 1]) = 1 - \lambda_d(s) dt - \lambda_u(s) dt. \quad (7)$$

That is, η is the probability of switching from the non-pandemic regime to the pandemic regime, and λ_d and λ_u are the respective probabilities in a pandemic state to move “down” or “up” to the adjacent states. Given this specification, a straightforward Markov chain calculation yields $\mathbb{E}_t[T^* | s]$ where T^* is the time at which the state S is attained and the pandemic is terminated.

The model’s depiction of the pandemic consists of a state-specific stochastic process for the accumulation of wealth. Specifically, let q denote the quantity of productive capital of an individual household (which could be viewed as both physical and human capital, potentially reflecting the health of the latter). We assume that the stock of q is freely convertible into a flow of consumption goods at rate C per unit time. Then our specification is that q evolves according to the process

$$dq = \mu(s)qdt - Cdt + \sigma(s)qdB_t - \chi(s)q dJ_t \quad (8)$$

where B_t is a standard Brownian Motion and J_t is a Poisson process with intensity $\zeta(s)$. We set $\chi(0) = \chi(S) = 0$ and $\chi(s) > 0$ for pandemic states. Hence we interpret the Poisson shock as capturing the risk of an economic loss when the household is hit by a “health disaster”. In non-pandemic states, $\mu(0) = \mu(S)$ and $\sigma(0) = \sigma(S)$ are the percentage growth rate (before consumption) and volatility of the wealth stock. In Section 5.2, we generalize the model to include a production function with optimal labor choice, thus endogenizing the difference between pandemic and non-pandemic output. To connect to our empirical work, however, we can work with the model in reduced-form.

Although the specification allows for arbitrary parameter differences across the pandemic states (hence potentially capturing diverse aspects of the pandemic), our intention

is rather to interpret the states as differing *only* in so far as advances in the state reduce the expected time to exit the pandemic, since the latter is the quantity that we attempt to measure in the data. Hence, for $0 < s < S$, we will take $\mu(s) = \mu(1)$, $\sigma(s) = \sigma(1)$, and $\chi(s) = \chi, \zeta(s) = \zeta$ to all be constants.

It is worth noting explicitly that our model does not include state variables that represent the dynamics of an infectious disease within the population, as in standard compartmental models. Obviously these dynamics matter for households and investors. However, purely from a descriptive standpoint, prior to the widespread deployment of vaccines, the degree of infectiousness in the U.S. (and elsewhere) was essentially unrelated to the degree of progress on vaccine research. So adding this layer of complexity would result in asset price variation that is orthogonal to the variation we measure empirically.

4.2 Agents

We assume the economy has a unit mass of identical agents (households). Each agent has stochastic differential utility or Epstein-Zin preferences (Duffie and Epstein, 1992; Duffie and Skiadas, 1994) based on consumption flow rate C , given as

$$\mathbb{J}_t = \mathbb{E}_t \left[\int_t^\infty f(C_{t'}, \mathbb{J}_{t'}) dt' \right] \quad (9)$$

and aggregator

$$f(C, \mathbb{J}) = \frac{\rho}{1 - \psi^{-1}} \left[\frac{C^{1-\psi^{-1}} - [(1-\gamma)\mathbb{J}]^{\frac{1}{\theta}}}{[(1-\gamma)\mathbb{J}]^{\frac{1}{\theta}-1}} \right] \quad (10)$$

where $0 < \rho < 1$ is the discount factor, $\gamma \geq 0$ is the coefficient of relative risk aversion (RRA), $\psi \geq 0$ is the elasticity of intertemporal substitution (EIS), and

$$\theta^{-1} \equiv \frac{1 - \psi^{-1}}{1 - \gamma} \quad (11)$$

The use of recursive preferences is standard in macrofinance models because of their ability to match financial moments. We recognize the limitations of using a utility specification driven by consumption goods, particularly within a crisis when other consider-

ations (e.g., health, social interaction, the safety of others) so strongly affect well-being. However, using a familiar formulation ensures that our findings are not driven by non-standard assumptions about utility. Another potentially restrictive assumption, given the myriad uncertainties during 2020 about the coronavirus itself, is that agents have complete knowledge of the stochastic properties of the pandemic. In Section 5, we will consider uncertainty about the transition probabilities for a two-state version of the model.

The representative agent's problem is, in each state s , to choose optimal consumption $C(s)$ that maximizes the objective function $\mathbf{J}(s)$. Section 5 will examine another extension in which the agent possesses a vaccine research technology and optimally chooses the rate of research expense.

4.2.1 Solution

We now characterize the solution to the optimization problem.

Proposition 1. *Denote*

$$g(s) \equiv \frac{(1-\gamma)\rho}{(1-\psi^{-1})} - (1-\gamma) \left(\mu(s) - \frac{1}{2}\gamma\sigma(s)^2 \right) - \left([1-\chi(s)]^{1-\gamma} - 1 \right) \quad (12)$$

Let $H(s)$'s denote the solution to the following system of S recursive equations:

$$g_0 \equiv g(0) = \frac{(1-\gamma)}{(\psi-1)} \rho^\psi (H(0))^{-\psi\theta^{-1}} + \eta \left[\frac{H(1)}{H(0)} - 1 \right] \quad (13)$$

$$g_1 \equiv g(1) = \frac{(1-\gamma)}{(\psi-1)} \rho^\psi (H(s))^{-\psi\theta^{-1}} + \lambda_d \left[\frac{H(s-1)}{H(s)} - 1 \right] + \lambda_u \left[\frac{H(s+1)}{H(s)} - 1 \right], \quad (14)$$

for $s \in \{1, \dots, S-1\}$.

Assuming the solutions are positive, optimal consumption in state s is

$$C(s) = \frac{(H(s))^{-\psi\theta^{-1}} q}{\rho^{-\psi}}, \quad (15)$$

and the value function of the representative agent is

$$\mathbf{J}(s) \equiv \frac{H(s)q^{1-\gamma}}{1-\gamma} \quad (16)$$

Note: All proofs appear in the appendix.

The recursive system is straightforward to solve numerically.³⁴ Henceforth we implicitly assume the parameters are such that a unique solution vector $H(s)$ exists and is strictly positive.³⁵ An important observation for our calibration exercise is that the pandemic parameters only affect the system (and hence its solution) through the constant g_1 . More generally, the solution depends on the relative values of g_0 and g_1 . The lower is g_1 relative to g_0 , the lower is the value function in pandemic states relative to the non-pandemic state. This difference in welfare values is the basis for our quantification of the value of a cure.

4.2.2 Value of a Cure

We define the value of a cure as the certainty equivalent change in the representative agent's lifetime value function upon a transition from state s to state 0 (or to state S):

$$V(s) = 1 - \left(\frac{H(s)}{H(0)} \right)^{\frac{1}{1-\gamma}} \quad (17)$$

This is the percentage of the agent's stock of wealth q that, if surrendered, would be fully compensated by the utility gain of reverting to the non-pandemic state. This willingness-to-pay definition is standard in the literature, since Lucas (1987). In Section 4.5 we compare our findings to work using the same definition to quantify the value of averting other types of disasters. Using the optimal consumption characterized above, we also obtain that

Proposition 2. *The value of a cure in the pandemic state s is determined by the ratio of marginal propensity to consume ($c \equiv dC/dq$) in the pandemic state s relative to that in the non-pandemic*

³⁴In the Appendix, we work out in detail the solution to the 2-state regime-switching model in which the pandemic regime consists of just one state. Besides illustrating the detailed solution to the model (Hamilton-Jacobi-Bellman (HJB) equations, labor and consumption choices, and system to determine the value function), it also serves as the benchmark case for developing the model further with parameter uncertainty.

³⁵A necessary and sufficient condition for this in the two-regime case is that $g_1 < g_0$.

state, adjusted by the agent's elasticity of intertemporal substitution (EIS):

$$V(s) = 1 - \left(\frac{c(s)}{c(0)} \right)^{-\frac{1}{\psi-1}} = 1 - \left(\frac{C(s)}{C(0)} \right)^{-\frac{1}{\psi-1}} \quad (18)$$

We will estimate this quantity below, under standard assumptions about the non-pandemic parameters, utilizing the information from our empirical exercise to restrict the set of pandemic parameters.

4.3 Asset Pricing

Our next step is to examine the model's counterpart to the sensitivity that we estimated in Section 3.2. We begin by interpreting "the market portfolio" within the model as a claim to the economy's output.³⁶ Output is the net new resources per unit time, which is implicitly defined by two endogenous quantities: the change in the cumulative wealth plus consumption, or $dq + Cdt$. Denote the price of the output claim as $P = P(s, q)$. By the fundamental theorem of asset pricing, the instantaneous expected excess return to holding this claim is equal to minus the covariance of its returns with the pricing kernel. Under stochastic differential utility, and with the value function solution above, the pricing kernel in our economy is given by

$$\Lambda_t = \exp \left\{ \int_0^t \left[\rho^\psi (\theta/\psi) H(s_u)^{-\psi/\theta} \right] du \right\} q_t^{-\gamma} H(s_t)$$

From this, we derive the value of the claim in the following proposition.

Proposition 3. *The price of the output claim is $P = p(s)q$ where the constants $p(s)$ solve a matrix system $Y = Xp$ where X is an $S+1$ -by- $S+1$ matrix and Y is an $S+1$ vector both of whose elements are given in the appendix.*

Henceforth we assume the model parameters are such that the matrix X defined

³⁶Note that this is not the same as a claim to aggregate consumption. As is well known (see Ai (2010)), in an economy where the capital stock can be costlessly converted to consumption goods, the consumption claim's price is equal to the capital stock, q . However, any wedge between consumption and payouts to equity will result in a nonconstant price-capital ratio. Our assumption here is that the expected cash flow to the market portfolio mirrors the expected impact of the pandemic on wealth. In Appendix ?? we describe a decentralization of the economy in which this cash flow is the net payout of the corporate sector to households.

in the proposition is of full rank. The behavior of the price-capital ratio, $p(s)$, accords with economic intuition: it declines sharply on a move from state $s = 0$ to $s = 1$, and then gradually (and approximately linearly) recovers as s advances. Thus, the quantity $\Delta \log P = \log p(s+1) - \log p(s)$ is positive for $s > 0$ and, in practice, varies little with s .

Next, define T^* as the time at which the state S is attained and the pandemic is terminated. Assuming the progression and regression intensities λ_u and λ_d are constant, it is straightforward to show that its time t expectation, $\mathbb{E}_t[T^*]$ is again given by a linear system, which we omit for brevity. Moreover, for large S , the difference

$$\Delta \mathbb{E}[T^*] = \mathbb{E}[T^*|s+1] - \mathbb{E}[T^*|s] \sim \frac{1}{\lambda_u} \quad (19)$$

is effectively constant as well.

Combining the above two results, we can readily define the model's analogue of the sensitivity that we empirically estimated as

$$\frac{\Delta \log P}{\Delta \mathbb{E}[T^*]}. \quad (20)$$

For our purposes the crucial property of this quantity, as we explain below, is it allows us to approximately pin down the pandemic parameters that determine the value of a cure.

4.4 Calibration and the Value of a Cure

In this section and the next, we present comparative static results exploring the determinants of the value of a cure, V , as defined in Section 4.2.2. In doing this, our approach is to fix the preference and non-pandemic output parameters, and infer the parameters governing the pandemic from the implied quantity (20).

The former set are taken to be relatively standard values, whose effects on the non-pandemic economy are well understood. Unless otherwise stated, we will fix these to be the values shown in Table 4. The preference parameters are broadly consistent with the macro-finance literature under stochastic differential utility, although we use a relatively low level of risk aversion. The growth rate and volatility parameters for the wealth stock are chosen to approximately match the growth rate and volatility of aggregate dividends in normal times, consistent with our interpretation of a claim to this stream as

representing the market portfolio.

The crucial quantity for our calibration is the *relative* loss of output during the pandemic. Specifically, asset markets are highly informative about the decline in the expected growth rate of the stock of wealth, $dq/q - Cdt$, under the risk-neutral measure. This rate of loss, which we denote Δm_Q , is driven primarily by the difference $\mu(1) - \mu(0)$ and by the expected intensity, $\chi\zeta$, of the Poisson health shocks. (The level of risk aversion and the Gaussian volatility play smaller roles, via the change of measure.) This is illustrated by the left panel in Figure 6, which plots the sensitivity of market returns to vaccine progress, (20), for a wide range of model solutions that differ in their values of the pandemic parameters. The plot shows that there is effectively a one-dimensional relationship between the market sensitivity and Δm_Q . Further, the middle panel shows that Δm_Q is itself tightly linked to the model parameter g_1 , which we showed above was a sufficient statistic for the value of a cure, given the non-pandemic parameters. This latter relationship is shown in figure's right hand panel.

Our estimated values for the market sensitivity in Table 2 using the KPSS methodology ranged from 0.041 to 0.064.³⁷ Using this range, the plots in Figure 6 imply a range of Δm_Q of approximately 0.045 to 0.065, implying g_1 in the range of -0.41 to -0.33. This, in turn, implies a value of the cure in the range of 6.5 to 9.0 percent of wealth.

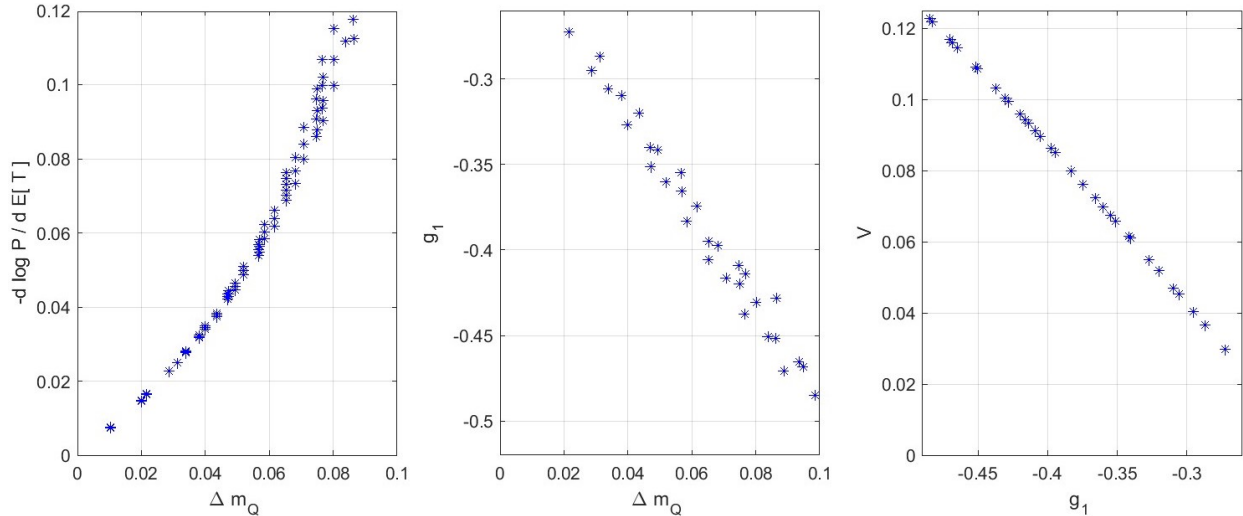
The above calculations assume specific values for the timing parameters. In particular, consistent with our empirical work, Figure 6 fixes the unconditional expected duration of the pandemic to be 4 years, and the current expected time to exit to be 2 years, corresponding to our estimate of the actual value in the early spring of 2020. The figure also takes the pandemic frequency parameter to be $\eta = 0.03$.³⁸ These timing choices have little effect on the identification plot in the left panel and none at all on the relationship in the middle plot. But they do affect the value of a cure, given the pandemic parameters.

Figure 7 plots the value of the cure as a function of η and λ , fixing the pandemic pa-

³⁷Given the variation in point estimates across methodologies in Table 2 and Table 3 we acknowledge that the data are not inconsistent with a wider range of possible values.

³⁸In addition, the solutions in this section will take the number of states to be $S = 12$, which is arbitrary. Our results are not sensitive to the choice of the number of states, given the total expected duration of the pandemic. Hereafter we will denote $\lambda_u/(S+1)$ as λ without a subscript. We also set the intensity of regress to be $\lambda_d = 0$, which limits vaccine related volatility. This choice accords with actual experience: the research setbacks through the Fall of 2020 were few and had insignificant impacts on our empirical measure of progress.

Figure 6: Stock Market Sensitivity Pins Down the Value of a Cure



Note: Figure shows how the market reaction to vaccine progress, $-\Delta \log P / \Delta E[T^*]$, helps pin down the value of a cure, V , through the decline in expected growth rate of capital q in pandemic states, Δm_Q , g_1 as defined in (14), and other pandemic parameters. Each \star corresponds to a different set of pandemic parameters. The left panel shows the range of Δm_Q for a given value of $-\Delta \log P / \Delta E[T^*]$. The middle panel shows the range of g_1 for a given value of Δm_Q . And the right panel shows the range of V for a given value of g_1 . In all three panels, the unconditional expected duration of the pandemic is 4 years, the current expected time to exit is 2 years, intensity of switching to the pandemic state $\eta = 0.03$, and number of pandemic states $S = 12$. The pandemic parameters being varied are the expected output growth ($\mu(1)$), output volatility ($\sigma(1)$), and the size of the health shock ($\chi(1)$).

rameters consistent with the above identification.³⁹ The left panel plots V against $1/\lambda$ the expected duration of the pandemic, while the right panel uses the pandemic frequency η on the horizontal axis. (The left panel sets $\eta = 0.03$ and the right panel sets $\lambda = 0.5$. Both panels take the current state as $s = 1$.) The right panel shows that the value of a cure is actually lower when pandemics are more frequent. Recall that a “cure” here only applies to the current pandemic. A one-time cure is less valuable when a new one will be needed sooner.

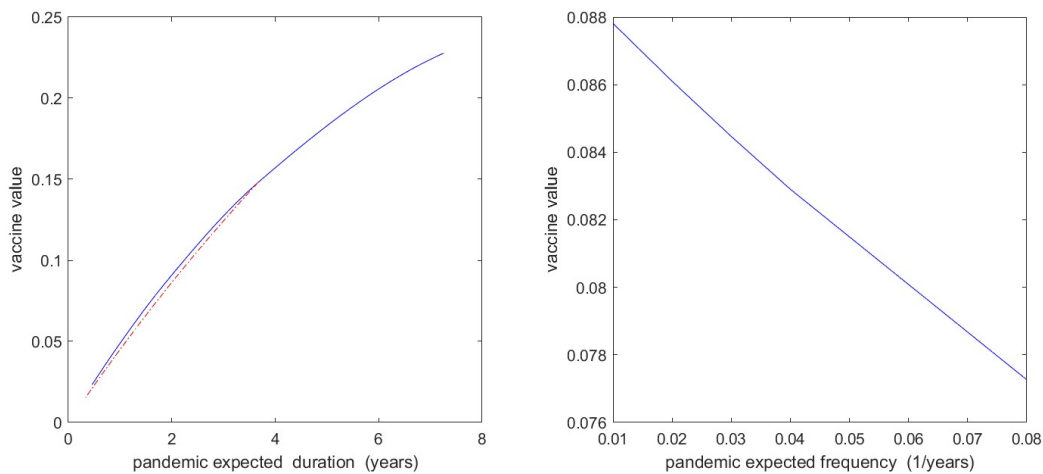
Comparing the panels, the model implies a much more important role for the expected duration of the pandemics than for their frequency. Intuitively, the output loss Δm_Q is a rate, and the value of a cure depends critically on how long that rate is expected to be experienced. The dashed line in the left-hand plot varies the expected duration by fixing λ and varying the current state, s . This line is almost identical to the solid one that

³⁹Specifically, the plot takes $\zeta = 1, \chi = 0.0475, \mu_1 = \mu_0, \sigma_1 = \sigma_0$. These imply $g_1 = -0.367$ and $\Delta m_Q = 0.0577$.

fixes s and varies λ , verifying that the precise combination of parameters is not important, given the forecast mean time, which is the quantity our VPI measures.

From the plot, agents in the economy would be willing to give up as much as 15% of their wealth for a cure when the pandemic is expected to last four years, as we estimate may have been the case in January 2020. In the crucial months of March and April, with our vaccine progress indicator falling towards one year, the figure implies a value of a cure of approximately 5% of total wealth. This 5-15% range – determined primarily by the range of expected duration – is our baseline finding. By November 2020, with less than six months expected until successful vaccine deployment, the cure was still worth over 2% of total wealth.

Figure 7: Value of a Cure



Note: Figure shows the value of a cure, V , as a function of the intensity of switching to the pandemic (non-pandemic) state η (λ). The left panel plots V against $1/\lambda$. The right panel plots V against η . The left panel sets $\eta = 0.03$ and the right panel sets $\lambda = 0.5$. The current state is set as $s = 1$.

4.5 Discussion

In assessing our conclusions on the value of a cure, two natural questions arise. First, how should one think about a valuation of “five percent of total wealth” in terms of real-world values (e.g., dollars)? Second, are these magnitudes reasonable?

On the first question, as a baseline value, total U.S. household wealth at the end of 2019 was approximately \$96 trillion, implying that five percent represents about \$5 trillion. However, some ambiguity arises in interpretation because of the stylized nature of

the model's depiction of wealth. A single state variable, q , represents not only household wealth, but the (book) value of the capital stock and the (market) value of a claim to all future dividends. One possibility is to view the magnitude of q through the lens of consumption. Aggregate U.S. nondurable and service consumption in 2019 was approximately \$13.4 trillion. In the model calibration, the marginal propensity to consume (C/q) is approximately 0.04,⁴⁰ which would imply that five percent of q represents (0.05/0.04) times C , or $V \approx \$17$ trillion.

We view numbers of \$5 trillion or more as plausible. The onset of the pandemic caused a decline in U.S. market capitalization – just one component of total wealth – of \$9 trillion. Likewise, our empirical estimates in Section 3 suggest that an increase in one year in expected duration of the pandemic decreases stock market wealth by around 6 percent. So sacrificing 6 percent of stock market wealth to avoid this outcome is a sensible exchange. The model simply fills in the missing steps by inferring the market's anticipation of the rate of loss of total wealth and translating that expectation into foregone utility.

Beyond the stock market, the suspension of economic activity caused by the pandemic created significant economic losses⁴¹ with reduced output, massive unemployment, reduced female labor force participation, and retooling/mothballing costs, for example. Fiscal response, designed in the scale of these losses, has amounted to almost \$6 trillion in the U.S., and on average over \$3 trillion and \$500 billion for G20 advanced economies and emerging markets, respectively.⁴² Economic activity can only resume with the widespread deployment of an efficacious vaccine, and CBO (2020) estimates over \$7 trillion in lost output through 2030 while Agarwal and Gopinath (2021) estimates an additional \$50 billion in facilitating vaccine availability would infuse \$9 trillion into the global

⁴⁰Our calibration follows Blundell et al. (2008), Souleles (1999) and Souleles (2002), among others.

⁴¹While the ex-post estimates of the cost of the pandemic is not equivalent to our estimates of the ex-ante value of a cure, the former is still insightful to the economic ramifications of a vaccine that ends the pandemic.

⁴²Data are from the IMF Database of Country Fiscal Measures in Response to the COVID-19 Pandemic and April 2021 World Economic Outlook. G20 advanced economics include Australia, Canada, France, Germany, Italy, Japan, South Korea, Spain, United Kingdom and United States. G20 emerging markets include Argentina, Brazil, China, India, Indonesia, Mexico, Russia, Saudi Arabia, South Africa and Turkey. Averages are weighted by GDP in USD and adjusted for purchasing power parity.

economy through 2025.⁴³

A recent literature also computes the welfare cost of eliminating the possibility of other types of disasters and their estimates are of similar order of magnitude.⁴⁴ Barro (2009) reports that, in a model with rare disasters, moderate risk aversion, and an EIS greater than one, society would be willing to pay up to 20% of permanent income to eliminate disaster risk. Tallarini Jr (2000) finds costs to reducing business cycle risk at 13% on the conservative end. And Pindyck and Wang (2013) estimates the willingness to pay to reduce the impact of a disaster to 15% of capital stock at 7%.

5 Extensions

We next examine some extensions of the model to highlight features absent in our reduced form that may make a vaccine or cure more or less valuable than our benchmark estimate.

5.1 Endogenous Vaccine Development

First, a potential criticism of the model is that it includes no actual vaccine development technology. The reason for this is simply that parameterizing and calibrating a bio-pharmaceutical R&D production function is beyond the scope of our study. However, there could be a concern that we overstate the value of ending the pandemic by not giving the economy a real option to address it. We now show a tractable way to do this, and we explain why our results are consistent with this extension. In a nutshell, optimal research effort will impose a constraint on the parameters that does not affect our empirical identification of the pandemic duration and severity.

Suppose that, when a pandemic arrives, the representative agent has the ability to choose an expenditure rate ι that increases the arrival rate of a cure. The most parsimonious specification would just be linear:

$$\lambda(\iota) = L_0 + L_1 \iota.$$

⁴³While our model does not incorporate the value of human life, Cutler and Summers (2020) augment CBO's projection with health losses caused by the pandemic and estimate the total economic cost of COVID-19 to be \$16 trillion.

⁴⁴Values are commonly reported as percentage reductions of permanent income. Such percentages are directly comparable to our percentages of (permanent) reductions in q since consumption is proportional to q .

(The discussion will treat the 2-state model. Generalization to S -states is straightforward.) Given the rate, the dynamics of wealth, dq/q , picks up a new term $-\iota dt$ for the duration of the pandemic. Without loss of generality, we can assert that whatever ι level the agent chooses in the first pandemic is also optimal for all subsequent pandemics. For notational simplicity below, define the adjusted drift during the pandemic as

$$\mu_S(\iota) = \mu(1) - \iota$$

where $\mu(1)$ is the benchmark growth rate without research effort. While this formulation is too sparse to address issues of public versus private returns to research expenditure, it does allow us to formulate and solve a model in which vaccine progress (and the attainment of a cure) is an endogenous outcome.

Notice that, given a choice of ι , the economy behaves exactly as in our reduced-form case. Hence the solution for optimal consumption and the value function are unchanged. In particular, we can write the value function within the pandemic as $H(1; \lambda(\iota), \mu_S(\iota))$. To choose the optimal policy, ι^* , the agent simply maximizes this function.⁴⁵ Of course, a necessary condition for an interior optimum is

$$\frac{\partial H}{\partial \mu_S} = L_1 \frac{\partial H}{\partial \lambda}.$$

Optimality of the research effort does constrain admissible pairs of λ and μ_S via this relation.

Clearly in an economy with powerful research technology (where L_1 is a large number), agents can make the pandemic very brief (in expectation) at low cost. Hence, the endogenous value of λ would be high, and agents would pay less for a cure than in an economy with inferior vaccine technology. However, recall that our benchmark calibration above already conditioned on different values of λ . We showed that the value of a cure depended strongly on the remaining expected duration of the pandemic, which could be inferred in the data from our estimation of the expected time to deployment of a vaccine during 2020.

⁴⁵This verifies that the optimal rate is constant within a state and does not vary across pandemics.

Now, taking λ as fixed at an observed value $\hat{\lambda}$ say, consider the ratio

$$f(\hat{\mu}_S) = \left. \frac{\partial H}{\partial \mu_S} \right|_{\hat{\lambda}, \hat{\mu}_S} / \left. \frac{\partial H}{\partial \lambda} \right|_{\hat{\lambda}, \hat{\mu}_S}.$$

Given any value of the technology parameter L_1 , the first order condition above requires us to use the value of $\hat{\mu}_S$ satisfying $f(\hat{\mu}_S) = L_1$. Assuming a solution exists, this is the full economic content of endogenizing vaccine investment in this setting.

Will imposing this restriction on μ_S affect our estimated value of a cure? To see why it will not, recall that the stock market response to vaccine progress pinned down the quantity that we called Δm_Q , the difference between the (risk neutral) expected growth rate of q in the pandemic and during normal times. As shown in Figure 6, this difference effectively determines V (via the intermediate quantity g_1) regardless of the values of the other pandemic parameters. Determining μ_S from the above first order condition does not change our empirical inference about Δm_Q .⁴⁶

To be clear, the conclusion is not that endogenizing vaccine development is unimportant in determining the value of a cure. Rather, we are pointing out that our empirical work has already determined (approximately) the key inputs to that value. Taking those quantities at face value, adding assumptions about the development technology and imposing the restriction of optimal investment do not perturb the calculation.

5.2 Endogenous Pandemic Severity and Labor Externalities

In this subsection, we propose a version of the model in which the pandemic parameters for the wealth process are endogenized through the choice of labor supply. Doing so will allow us to examine how much the value of a cure is influenced by the extent to which individual choices deviate from the socially optimal policies. The development here parallels Gourio (2012) with a few changes as noted earlier in the paper.

In this version of the model, wealth accumulates according the stochastic process

$$dq = \ell^\alpha q \mu dt - C dt + \sigma \ell^{\alpha/2} q dB_t \tag{21}$$

⁴⁶In terms of the model parameters, Δm_Q depends upon several things besides μ_S , including the expected health shocks per unit time and the degree of risk aversion.

in the non-pandemic state, and

$$dq = \ell^\alpha q \mu dt - C dt + \sigma \ell^{\alpha/2} q dB_t - [\ell \varepsilon + k + KL] q dJ_t. \quad (22)$$

in the pandemic state. As before, C is the endogenous consumption rate, and now ℓ is the household's labor supply, and $\alpha \in (0, 1)$ is the elasticity of expected output with respect to labor.⁴⁷ Crucially, both individual and aggregate labor are assumed to affect the agent's exposure to the health shock via the jump size. Let

$$\chi(\ell, L) \equiv [\ell \varepsilon + k + KL], \quad (23)$$

where ε is exposure to the pandemic via private labor, k is exposure to the pandemic unrelated to labor, L is aggregate labor supply, and K is exposure via aggregate labor. These parameters can capture losses of wealth due to health-induced disruptions to work, the need to work from home with attendant productivity impact and loss of human capital, deadweight losses from bankruptcy, and frictions from labor reallocation. We will assume parametric restrictions on ε , k and K to be small enough that $(1 - \chi) \in (0, 1)$. The agent takes the aggregate supply of labor L as given in her optimization problem.

Agents' preferences are as in Section 4.2. We assume no disutility to labor supply and no frictions in adjusting ℓ . We assume $\ell \in [0, \bar{\ell}]$, where the upper bound $\bar{\ell}$ is the agents' total available work capacity. (In the numerical work we normalize $\bar{\ell} = 1$.)

The agent's problem is now to choose in each state s optimal consumption $C(s, L^*(s))$ and labor $\ell(s, L^*(s))$ that maximizes the objective function. We impose that agents have rational expectations about $L^*(s)$, the aggregate labor in equilibrium. In other words, individual agents' decisions in the aggregate should lead to a wealth (consumption) dynamic that is confirmed in equilibrium. This implies the following for wealth dynamics in the pandemic regime:

$$dq(s) = [\ell(s, L^*(s))]^\alpha q \mu dt - C(s, L^*(s)) dt + \sigma [\ell(s, L^*(s))]^{\alpha/2} q dB - \chi(\ell(s, L^*(s)), L^*(s)) q dJ_t \quad (24)$$

Since $L^*(s)$ is a constant for each s , as the agent has rational expectations about $L^*(s)$, the

⁴⁷The results below all go through with constant returns to scale in the drift term.

above dynamics are identical to those assumed by the agent. Substituting for the equilibrium fixed point that $L^*(s) = \ell(s, L^*(s))$, we can then obtain the rational expectations equilibrium outcomes.

Proposition 4. *Equilibrium labor in the non-pandemic state is given by*

$$L(0) = L(S) = \bar{\ell} \quad (25)$$

Equilibrium labor in pandemic states $L^(s) \forall s \in \{1, \dots, S-1\}$ solves⁴⁸*

$$\chi(L(s), L(s)) = k + (\varepsilon + K)L(s) = \left[1 - (L(s))^{\frac{1-\alpha}{\gamma}} \nu\right] \quad (27)$$

where

$$\nu \equiv \left[\frac{\alpha \left(\mu - \frac{1}{2} \gamma \sigma^2 \right)}{\zeta \varepsilon} \right]^{-\frac{1}{\gamma}}. \quad (28)$$

In the non-pandemic state, the agent faces no cost to supplying labor and exerts effort fully. However, in the pandemic states, the agent increases exposure to health risk by supplying labor, which creates a tradeoff between augmenting the capital stock and reducing the loss of capital that arises from health shocks. A key property of the model is that the agent contracts labor relative to the non-pandemic state.

Note the externality in our set up via the KL term in the size of the Poisson shock (where L is aggregate labor) that is not internalized by each agent. A central planner would factor this in the socially efficient choice of labor. This is tantamount to replacing ε

⁴⁸It can be shown that given $\alpha \in (0, 1)$, the second order condition for a maximum is satisfied whenever

$$\mu - \frac{1}{2} \gamma \sigma^2 > 0 \quad (26)$$

which also implies $\nu > 0$.

by $(\varepsilon + K)$ in ν above to obtain ν^{CP} :

$$\nu^{CP} \equiv \left[\frac{\alpha \left(\mu - \frac{1}{2} \gamma \sigma^2 \right)}{\zeta(\varepsilon + K)} \right]^{-\frac{1}{\gamma}} \quad (29)$$

Socially efficient labor choice $L^{CP}(s)$ in the pandemic states is then given by

$$\chi(L(s), L(s)) = k + (\varepsilon + K)L(s) = \left[1 - (L(s))^{\frac{1-\alpha}{\gamma}} \nu^{CP} \right] \quad (30)$$

It is then straightforward to show that $\nu^{CP} > \nu$ for $K > 0$ and $\gamma > 0$, and hence $L^{CP}(s) < L(s)$, i.e., the socially efficient choice of labor in pandemic states is smaller than the privately optimal one.

Given the optimal labor and consumption policies, the model solutions in Proposition 1 can be directly applied. As before, the pandemic parameters only enter the system of equations via the constants g_0 and g_1 , which we can write compactly as

$$g(x, y) \equiv \frac{(1 - \gamma)\rho}{(1 - \psi^{-1})} - x^\alpha (1 - \gamma) \left(\mu - \frac{1}{2} \gamma \sigma^2 \right) - y \left([1 - \chi(x, x)]^{1-\gamma} - 1 \right) \quad (31)$$

with $g_0 = g(\bar{\ell}, 0)$ and $g_1 = g(\ell(s), \zeta)$.

To quantitatively evaluate the model's implications, we require that the parameters are such that the endogenous severity of the pandemic is in line with our empirical estimates. To this end we report the implied Δm_Q for a range of values of K and ε ⁴⁹ in Table 5. Recall, our empirical estimates suggested a value for this quantity in the range of 0.05-0.06. We also report the optimal labor supply in the pandemic state, ℓ^* . Some empirical evidence suggests labor contraction $\approx 20\%$ in April 2020 (Cajner et al. (2020)) corresponding to $\ell^* \approx 0.80$. The table identifies parameter regions (e.g., the upper left of the tables)

⁴⁹The exercise fixes α and k . These parameters have less direct impact on the degree of labor externality.

that can match both restrictions.^{50,51}

Table 6 shows the effect on V of the labor market externality for the same range of parameter values. The left panel provides a direct measure of the scale of the externality via the ratio of the central planner’s solution for optimal labor in the pandemic to that actually chosen by agents. With parameters in the region identified above, the socially optimal lockdown is quite severe with labor restricted to 30%-40% of the privately optimal amount.⁵² The right panel shows that, in this region, the value of a cure is 12%-19% lower under the central planner’s solution.⁵³

In addition to the finding that a cure is less valuable under a central planner, comparing variation across the two panels reveals the pattern that a stronger externality (as measured by lower values of ℓ_{cp}^*/ℓ^*) are associated with decreasing relative values for a cure under the central planner. In effect, the extra degree of lockdown that the planner would impose and the vaccine are substitutes as countermeasures. We acknowledge that if the arrival of the pandemic were to result in social costs that are outside the capital stock dynamics for the agent, then the planner might value the vaccine more than the representative agent.

⁵⁰Using customized survey data, Coibion et al. (2020a,b) find the pandemic led to a 20 million decline in the number of employed workers by the first week of April 2020, and attributed 60% of the decline in the employment-to-population ratio by May 2020 to lockdowns. Dingel and Neiman (2020), Mongey et al. (2020) and Beland et al. (2020) document more adverse labor market outcomes for occupations with high proximity among coworkers, or low work from home feasibility. For those looking for employment, Forsythe et al. (2020) find job vacancies had fallen 40% by April 2020 compared to pre-COVID-19 levels, with the largest declines in leisure, hospitality and non-essential retail.

⁵¹Baker et al. (2020a) deploy transaction-level data to study consumption responses to the pandemic, finding an increase in the beginning in an attempt to stockpile home goods, followed by a sharp decrease as the virus spread and stay at home orders were enforced. Using customized survey data, Coibion et al. (2020a) find lockdowns decreased consumer spending by 30 percent, with the largest drops in travel and clothing. Chetty et al. (2020) further find high-income households significantly reduced spending, especially on services that require in-person interactions, leading to business losses and layoffs in the most affluent neighborhoods. Outside the US, Sheridan et al. (2020) and Andersen et al. (2020) find aggregate spending decreased 27% in the first seven weeks following Denmark’s shutdown, with the majority of the decline caused by the virus itself regardless of social distancing laws.

⁵²While our model does not feature SIR dynamics, models with SIR dynamics and labor externalities generally see more severe lockdown policies under a central planner (see Abel and Panageas (2021)).

⁵³In our setting, the central planner is able to actually specify a level of labor contraction that is state-dependent. In reality, it is a discrete decision based on the realized severity.

5.3 Learning and Uncertainty

We have used the S -state version of our model to study the reaction of markets to vaccine news within a pandemic. Relating its predictions to the empirical evidence in Section 3 has provided evidence on plausible parameters affecting the value of a vaccine. Now we return to the two-state version of our model in order to examine the role of vaccine news from a different angle. Specifically, we are interested in the accumulation of information over longer horizons about the frequency and duration of pandemics. We study the effect upon the value of a vaccine of uncertainty about these quantities and of differing attitudes towards uncertainty.

5.3.1 Information Structure

Recall that in the two-state model η is the intensity of switching from state 0 (“off”) to state 1 (“on”) and λ is the intensity of switching from 1 to 0. In this section, we assume that agents have imperfect information about these intensities.

Let us stipulate that at time zero the agent has beliefs about the two parameters that are described by gamma distributions, which are independent of each other. Each gamma distribution has a pair of non-negative hyperparameters, a^η, b^η and a^λ, b^λ , that are related to the first and second moments via

$$\mathbb{E}[\eta] = \frac{a^\eta}{b^\eta}, \quad \text{Std}[\eta] = \frac{\sqrt{a^\eta}}{b^\eta}, \quad (32)$$

and likewise for λ .

By Bayes’ rule, under this specification, as the agent observes the switches from one regime to the next, her beliefs remain in the gamma class with the hyperparameters updating as follows

$$\begin{aligned} a_t^\eta &= a_0^\eta + N_t^\eta \\ b_t^\eta &= b_0^\eta + t^\eta \end{aligned}$$

where t^η represents the cumulative time spent in state 0 and N_t^η represents the total number of observed switches from 0 to 1. Analogous expressions apply for λ . Thus, during the “off” regime, the only information that arrives (on a given day, say) is whether or not

we have switched to “on” on that day. If that has occurred, the counter N^η increments by one and the clock t^η turns off (and t^λ turns on). In this version of the model, that is the entirety of the information revelation. In contrast to the previous section, no good or bad news arrives about progress during a regime. Although this setting lessens the model’s ability to speak to high-frequency dynamics, it allows us to study the role of uncertainty in the economy’s longer term evolution.

Under the above information structure, the economy is characterized by a six-dimensional state vector consisting of the stock of wealth, q , $a^\eta, b^\eta, a^\lambda, b^\lambda$ and the regime indicator S . However this six-dimensional space can actually be reduced to three.

Since the switches between states alternate, let us define an integer index M_t to be the total number of switches $N_t^\eta + N_t^\lambda$ and then (assuming we are in state 0 at time 0) $N_t^\eta = M_t/2$ when M is even, and $N_t^\lambda = (M_t + 1)/2$ when M is odd. Knowing M (along with the priors a_0^η and a_0^λ) is equivalent to knowing a_t^η and a_t^λ . Given these values, specifying the current estimates

$$\hat{\eta}_t \equiv \mathbb{E}_t[\eta] \quad \text{and} \quad \hat{\lambda}_t \equiv \mathbb{E}_t[\lambda] \quad (33)$$

is equivalent to specifying the remaining hyperparameters b_t^η and b_t^λ . Thus, solutions to the model can be described as a sequence of functions $H_M(\hat{\eta}, \hat{\lambda})$ for the agent’s value function at step M .

Compared to the full-information model in Section 4, within each regime the only new changes to the state come through variation in the estimates $\hat{\eta}_t$ and $\hat{\lambda}_t$ which change deterministically with the respective clocks t^η and t^λ . Holding M fixed, the dynamics of $\hat{\eta}_t$ are given by

$$d\hat{\eta}_t = d \frac{a_t^\eta}{b_t^\eta} = a_t^\eta d \frac{1}{b_t^\eta} \quad (34)$$

$$= - \frac{a_t^\eta}{(b_t^\eta)^2} dt \quad (35)$$

$$= - \frac{(\hat{\eta}_t)^2}{a_t^\eta} dt. \quad (36)$$

Under partial information, we proceed as in Section 4 to write-out the HJB equation

with the state variables following the dynamics determined by the representative agent's information set. As before, we can conjecture a form of the value function

$$\mathbf{J} = \frac{q^{1-\gamma}}{1-\gamma} H(\hat{\eta}, \hat{\lambda}, M; C, \ell). \quad (37)$$

And, as before the first order condition for consumption yields $C = q (\rho^\psi) H_1^e$ (where e_1 is defined in Section 4.1). This follows because consumption does not enter into any of the new terms involving the information variables. Also fortunately, none of the information variables appears in terms affected by labor supply, ℓ , and the function H drops out of the first-order condition for ℓ . (Intuitively, nothing about the likelihood of changing regimes affects the optimal choice of labor within a regime.) This means that the solutions for ℓ^* can be computed independent of the rest of the system.

Using these the results, the HJB system can be written as the infinite-dimensional linked PDEs, where M runs over the even integers:⁵⁴

$$g_0 = \rho^\psi \left(\frac{\theta}{\psi} \right) H_M^{-\psi/\theta} + \hat{\eta} \left(\frac{H_{M+1}}{H_M} - 1 \right) - \frac{(\hat{\eta})^2}{a^\eta H_M} \frac{\partial H_M}{\partial \hat{\eta}} \quad (38)$$

$$g_1 = \rho^\psi \left(\frac{\theta}{\psi} \right) H_{M+1}^{-\psi/\theta} + \hat{\lambda} \left(\frac{H_{M+2}}{H_{M+1}} - 1 \right) - \frac{(\hat{\lambda})^2}{a^\lambda H_{M+1}} \frac{\partial H_{M+1}}{\partial \hat{\lambda}}. \quad (39)$$

For large M , the estimation errors for both η and λ , expressed as a fraction of the posterior estimates, go to zero:

$$\frac{\text{Std}[\eta]}{\mathbb{E}[\eta]} = \frac{1}{\sqrt{a^\eta}} = \frac{1}{\sqrt{a_0^\eta + M_t}}. \quad (40)$$

The system always converges to the full-information solution, providing a boundary condition, which, together with the single-regime solutions on the edges of the $(\hat{\eta}, \hat{\lambda})$ plane, enables computation of all individual H functions.⁵⁵ It can be shown that, as in the full-information case, a necessary and sufficient condition for existence of a solution is $g_0 > g_1$.

As in the previous section, once the value function is obtained, we can characterize

⁵⁴The constants g_0 and g_1 are as defined in Section 4. See the internet appendix for a derivation of (38)-(39).

⁵⁵Knowing the solution for higher M enables direct evaluation of the jump-terms in (38)-(39). Knowing the solution on the inner edges enables explicit approximation of the first partial derivatives.

the certainty equivalent value of a vaccine that produces an immediate transition from the pandemic state to the non-pandemic state. The next section performs this calculation and analyzes the drivers of variation in that value.

5.3.2 Results

Table 7 shows numerical solutions for the value of a vaccine using the benchmark parameters from Section 4 but varying the elasticity of intertemporal substitution (EIS). The upper two panels show the full-information solution, with the upper right case corresponding to the benchmark $\psi = 1.5$, whereas the left panel lower the EIS to $\psi = 0.15$. There is almost no difference between the two solutions (which verifies the robustness of the conclusions in Section 4 on this dimension). The bottom two panels show the results under partial information. Specifically, results are computed under the assumption that agents' standard deviation of beliefs about the two parameters are equal to their mean beliefs. Comparing the right-hand panels, we see that this degree of parameters uncertainty has the effect of raising the level of wealth agents in the economy would be willing to surrender for a cure in the baseline case of a high EIS by between 7 and 15 percentage points, or up to a factor of three times the full information value. The left hand panels show the same effect, but amplified to an extreme level. With a low intertemporal elasticity, the representative agent would be willing to sacrifice on the order of 50 to 60 percent of accumulated wealth.

An additional computation that our framework can address is the value of a permanent cure. Table 8 shows the fraction of wealth agents in the economy would exchange to live in a world with no pandemics. (Formally, this is equivalent to letting λ go to infinity.) As expected, the values now show the same pattern as in Table 7, but exaggerated still further. In this case, eliminating the threat *and* resolving the parameter uncertainty can lead to valuation of 25 to 50% for high EIS agents and 60 to 80 percent for low EIS agents.

The latter finding may be counterintuitive based on the common understanding of Epstein-Zin preferences under which agents with $\psi < 1/\gamma$ can be viewed as having a preference for "later resolution of uncertainty." In the current model, agents facing a pandemic are much worse off with parameter uncertainty. This is verified in Table 9 where we compute the value that agents would pay to resolve parameter uncertainty *without* ending the on-going pandemic.

For both values of EIS the numbers are again extremely high, and for the low EIS case they are even higher than in the previous table. Apparently, in this economy, low-EIS agents would pay dearly for early resolution of uncertainty. The source of the extreme welfare loss in this case is the endogenous consumption response. Recall that low-EIS agents cut their consumption during a pandemic. With parameter uncertainty this response becomes extreme because agents cannot rule out the worst case scenario that $\lambda \sim 0$, i.e., that there will be a cure and the pandemic effectively lasts forever. This possibility leads to extreme savings and, consequently, little utility flow from consumption.

Even with high EIS however, the effect of parameter uncertainty is economically large, and is again due to agents being unable to rule out worst-case scenarios. From a policy perspective, the implication of this finding is that, while working to end the current pandemic is enormously valuable, equally and perhaps even more valuable is anything that resolves uncertainty about the frequency and, especially, the duration of current and future pandemics. In addition to developing cures and vaccines, understanding the fundamental science behind the fight against viral pathogens and investing in the infrastructure for future responses can provide crucial gains to welfare.

6 Conclusion

This paper provides an estimate of the value of a “cure” – a means of ending a pandemic – using the joint behavior of stock prices and a novel vaccine progress indicator based on the chronology of stage-by-stage advance of individual vaccine candidates and related news during 2020. In the context of a general equilibrium regime-switching model of repeated pandemics, the sensitivity of stock prices to vaccine progress indicator is essentially determined by the expected rate of loss (or lower growth rate) of wealth during a pandemic. Our empirical estimate can thus be translated into an implied welfare gain attributable to a cure. With standard preferences parameters, the value of a cure turns out to be worth approximately 5-15% of wealth, depending mainly on the expected remaining duration of the pandemic.

We extend the model to endogenize vaccine research and show that our results are robust to this generalization. We also endogenize the degree of pandemic severity by including labor choice, which affects agents’ exposure to the virus. When agents do not internalize the effect of their exposure choice on the economy’s overall exposure, the value

of a cure rises relative to central planning. In effect, the socially optimal lockdown policy lessens the welfare improvement due to exiting the pandemic.

We also show that the value of the cure rises sharply when there is uncertainty about the stochastic parameters governing the frequency and duration of pandemics. Indeed, we find that the representative agent would be willing to pay as much for resolution of this parameter uncertainty as for the cure itself. An important policy implication is that understanding the fundamental biological and social determinants of future pandemics, for instance, whether pandemics are related to zoonotic diseases triggered more frequently by climate change, may be as important to mitigating their economic impact as resolving an immediate pandemic-induced crisis.

References

- Andrew Abel and Stavros Panageas. Social distancing, vaccination and the paradoxical optimality of an endemic equilibrium. Technical report, Working Paper, 2021.
- Ruchi Agarwal and Gita Gopinath. A proposal to end the covid-19 pandemic. Technical report, IMF Staff Discussion Notes no. 2021/004, 2021.
- Hengjie Ai. Information quality and long-run risk: Asset pricing implications. *The Journal of Finance*, 65(4):1333–1367, 2010.
- Fernando Alvarez and Urban J Jermann. Using asset prices to measure the cost of business cycles. *Journal of Political economy*, 112(6):1223–1256, 2004.
- Asger Lau Andersen, Emil Toft Hansen, Niels Johannesen, and Adam Sheridan. Consumer responses to the covid-19 crisis: Evidence from bank account transaction data. Technical report, CEPR, April 2020.
- Scott Baker, R.A. Farrokhnia, Steffen Meyer, Michaela Pagel, and Constantine Yannelis. How does household spending respond to an epidemic? consumption during the 2020 covid-19 pandemic. *NBER Working Paper*, 2020a.
- Scott R Baker, Nicholas Bloom, Steven J Davis, Kyle Kost, Marco Sammon, and Tasaneeya Viratyosin. The Unprecedented Stock Market Reaction to COVID-19. *The Review of Asset Pricing Studies*, 07 2020b.
- Robert J. Barro. Rare Disasters and Asset Markets in the Twentieth Century*. *The Quarterly Journal of Economics*, 121(3):823–866, 08 2006.
- Robert J Barro. Rare disasters, asset prices, and welfare costs. *American Economic Review*, 99(1):243–64, 2009.
- Louis-Philippe Beland, Abel Brodeur, and Taylor Wright. Covid-19, stay-at-home orders and employment: Evidence from cps data. Working Paper 13282, IZA Institute of Labor Economics, May 2020.
- Richard Blundell, Luigi Pistaferri, and Ian Preston. Consumption inequality and partial insurance. *American Economic Review*, 98(5):1887–1921, December 2008.
- CBO. An update to the economic outlook: 2020 to 2030. Technical report, 2020.
- Raj Chetty, John N Friedman, Nathaniel Hendren, Michael Stepner, and The Opportunity Insights Team. How did covid-19 and stabilization policies affect spending and employment? a new real-time economic tracker based on private sector data. Working Paper 27431, National Bureau of Economic Research, June 2020.

- Olivier Coibion, Yuriy Gorodnichenko, and Michael Weber. The cost of the covid-19 crisis: Lockdowns, macroeconomic expectations, and consumer spending. Working Paper 27141, National Bureau of Economic Research, May 2020a.
- Olivier Coibion, Yuriy Gorodnichenko, and Michael Weber. Labor markets during the covid-19 crisis: A preliminary view. Working Paper 27017, National Bureau of Economic Research, April 2020b.
- Pierre Collin-Dufresne, Michael Johannes, and Lars A. Lochstoer. Parameter learning in general equilibrium: The asset pricing implications. *American Economic Review*, 106(3): 664–98, March 2016.
- Mariano M Croce, Thien T Nguyen, and Lukas Schmid. The market price of fiscal uncertainty. *Journal of Monetary Economics*, 59(5):401–416, 2012.
- David M. Cutler and Lawrence H. Summers. The COVID-19 Pandemic and the \$16 Trillion Virus. *JAMA*, 324(15):1495–1496, 10 2020.
- Jonathan I Dingel and Brent Neiman. How many jobs can be done at home? Working Paper 26948, National Bureau of Economic Research, April 2020.
- Darrell Duffie and Larry G. Epstein. Asset pricing with stochastic differential utility. 5: 411–436, 1992.
- Darrell Duffie and Costis Skiadas. Continuous-time security pricing: A utility gradient approach. *Journal of Mathematical Economics*, 23:107–132, 1994.
- Vadim Elenev, Tim Landvoigt, and Stijn Van Nieuwerburgh. Can the covid bailouts save the economy. Technical report, CEPR working Paper DP14714, 2020.
- Eliza Forsythe, Lisa B Kahn, Fabian Lange, and David G Wiczer. Labor demand in the time of covid-19: Evidence from vacancy postings and ui claims. Working Paper 27061, National Bureau of Economic Research, April 2020.
- X. Gabaix. Variable rare disasters: An exactly solved framework for ten puzzles in macro-finance. *Quarterly Journal of Economics*, 127(2):645–700, 2012.
- Niels Joachim Gormsen and Ralph S J Koijen. Coronavirus: Impact on Stock Prices and Growth Expectations. *The Review of Asset Pricing Studies*, 10(4):574–597, 09 2020.
- François Gourio. Disaster risk and business cycles. *American Economic Review*, 102(6): 2734–66, May 2012.
- Harrison Hong, Jeffrey Kubik, Neng Wang, Xiao Xu, and Jinqiang Yang. Pandemics, vaccines and corporate earnings. Technical report, Working Paper, 2020a.
- Harrison Hong, Neng Wang, and Jinqiang Yang. Implications of stochastic transmission rates for managing pandemic risks. Working Paper 27218, National Bureau of Economic Research, May 2020b.

- IMF. World economic outlook. Technical report, 2021.
- Raymond Kan and Cesare Robotti. On moments of folded and truncated multivariate normal distributions. *Journal of Computational and Graphical Statistics*, 26(4):930–934, 2017.
- Leonid Kogan, Dimitris Papanikolaou, Amit Seru, and Noah Stoffman. Technological innovation, resource allocation, and growth. *The Quarterly Journal of Economics*, 132(2): 665–712, 2017.
- Julian Kozlowski, Laura Veldkamp, and Venky Venkateswaran. Scarring body and mind: The long-term belief-scarring effects of covid-19. Technical report, 2020 Jackson Hole Economic Policy Symposium Proceedings, 2020.
- Robert Lucas. *Models of Business Cycles*. Blackwell, Oxford, 1987.
- Simon Mongey, Laura Pilossoph, and Alex Weinberg. Which workers bear the burden of social distancing policies? Working Paper 27085, National Bureau of Economic Research, May 2020.
- A. O’hagan. Bayes estimation of a convex quadratic. *Biometrika*, 60(3):565–571, 1973.
- Robert S. Pindyck and Neng Wang. The economic and policy consequences of catastrophes. *American Economic Journal: Economic Policy*, 5(4):306–39, November 2013.
- Adam Sheridan, Asger Lau Andersen, Emil Toft Hansen, and Niels Johannesen. Social distancing laws cause only small losses of economic activity during the covid-19 pandemic in scandinavia. *Proceedings of the National Academy of Sciences*, 117(34):20468–20473, 2020.
- Nicholas S. Souleles. The response of household consumption to income tax refunds. *American Economic Review*, 89(4):947–958, September 1999.
- Nicholas S Souleles. Consumer response to the reagan tax cuts. *Journal of Public Economics*, 85(1):99–120, 2002.
- Thomas D Tallarini Jr. Risk-sensitive real business cycles. *Journal of Monetary Economics*, 45(3):507–532, 2000.
- Jerry Tsai and Jessica A. Wachter. Disaster risk and its implications for asset pricing. *Annual Review of Financial Economics*, 7(1):219–252, 2015.
- Chi Heem Wong, Kien Wei Siah, and Andrew W Lo. Estimation of clinical trial success rates and related parameters. *Biostatistics*, 20(2):273–286, 01 2018.

Table 1: Forecast Comparison

<i>Deutsche Bank</i>			
Date	Survey median	VPI	% respondents below
May	1.158	0.958	35.0
June	1.162	0.893	31.2
July	0.920	0.595	20.8
Sep	0.625	0.561	44.3
<i>Superforecasters</i>			
Date	Survey median	VPI	% respondents below
April	1.902	1.291	16.1
May	1.603	0.958	14.6
June	1.189	0.893	31.0
July	0.808	0.595	32.7
August	0.519	0.606	58.4
September	0.445	0.518	57.2

Note: Table compares forecasts for the earliest date of vaccine availability in years. The top panel compares the median from a survey conducted by Deutsche Bank, while the bottom panel compares the median from a survey conducted by Good Judgement Inc. The column VPI denotes the forecast from our estimated vaccine progress indicator, and the last column reports the percent of respondents from each survey with forecasts below ours. Survey respondents are reported in calendar intervals. The comparison assumes a uniform distribution of forecasts in time within the median bin. The survey dates are as of the end of the month in the first column, except the Deutsche Bank September survey which is for the week ending September 11, 2020.

Table 2: Stock Market Sensitivity to Vaccine Progress

	(1) OLS	(2) KPSS (Prior 1)	(3) KPSS (Prior 2)
γ_1	-0.070 (0.067)	-0.088 (0.035)	-0.096 (0.035)
γ_2	0.131 (0.092)	0.163 (0.035)	0.168 (0.035)
β_{t-2}	1.316 (1.526)	-0.536 (0.423)	-0.382 (0.290)
β_{t-1}	-4.124 (3.121)	-1.924 (0.746)	-1.269 (0.586)
β_t	-1.100 (0.739)	-0.942 (0.592)	-0.991 (0.606)
β_{t+1}	0.719 (2.054)	-0.517 (0.412)	-0.432 (0.342)
β_{t+2}	-5.404 (1.729)	-2.446 (0.760)	-1.011 (0.458)
α	0.204 (0.097)	0.240 (0.079)	0.279 (0.078)
$\sum_{h=-2}^2 \beta_{t+h}$	-8.593 (0.653)	-6.365 (1.345)	-4.086 (1.056)
N	206	206	206

Note: Table shows the results from regression (1). The dependent variable is daily excess returns on the market portfolio in percent. Independent variables include two lags of excess returns on the market portfolio, a five-day window of changes in vaccine progress indicator in years, and dummy variables for each jump date from Baker et al. (2020b) unrelated to news about vaccine progress. The return on the value-weighted CRSP index is used from January 1, 2020 to October 31, 2020. All columns employ the baseline specification with news applying to all states, deterministic depreciation, base copula correlation of 0.2, probability of success in the application state equal to 0.95 and excludes candidates from China and Russia. Column 1 estimates the regression using OLS. Columns 2 and 3 employ the methodology of Kogan et al. (2017) and assume the pre-truncated normal distribution for β_t has standard deviation equal to 1. Column 2 further uses the same prior for all response coefficients, while column 3 uses a pre-truncated standard deviation of 0.7 for the first lead and lag and 0.5 for the second lead and lag. OLS results display Newey-West standard errors with four lags in parentheses and standard deviation of the F -statistic on $\sum_{h=-2}^2 \beta_{t+h}$. KPSS results show posterior standard deviations in parentheses.

Table 3: Stock Market Sensitivity to Vaccine Progress – Robustness

	(1)	(2)	(3)	(4)	(5)	(6)
News	All states	None	Current state	All states	All states	All states
Depreciation	Y	N	Y	Y	Y	Y
$\text{Cor}(n, n')$	0.2	0.2	0.2	0.4	0.2	0.2
$\pi_{\text{approval}}^{\text{base}}$	0.95	0.95	0.95	0.95	0.85	0.95
Ex-China and Russia	Y	Y	Y	Y	Y	N
γ_1	-0.070 (-1.04)	-0.067 (-1.01)	-0.068 (-1.02)	-0.075 (-1.10)	-0.073 (-1.08)	-0.080 (-1.50)
γ_2	0.131 (1.43)	0.116 (1.32)	0.127 (1.42)	0.131 (1.42)	0.134 (1.46)	0.111 (1.37)
β_{t-2}	1.316 (0.86)	2.389 (1.07)	1.543 (0.90)	1.275 (0.73)	0.959 (0.63)	1.980 (1.19)
β_{t-1}	-4.124 (-1.32)	-5.400 (-1.36)	-3.168 (-1.21)	-3.566 (-1.16)	-3.927 (-1.31)	-5.331* (-1.80)
β_t	-1.100 (-1.49)	-0.570 (-0.50)	-1.046 (-1.41)	-1.185 (-1.57)	-1.157 (-1.56)	1.084 (0.78)
β_{t+1}	0.719 (0.35)	2.085 (0.79)	1.112 (0.59)	0.807 (0.43)	0.600 (0.30)	-0.696 (-0.44)
β_{t+2}	-5.404*** (-3.13)	-7.310*** (-4.30)	-5.189*** (-3.65)	-4.872*** (-2.84)	-5.057*** (-2.72)	-4.171 (-1.61)
α	0.204** (2.11)	0.195* (1.94)	0.226** (2.28)	0.220** (2.27)	0.203** (2.11)	0.210** (2.14)
$\sum_{h=-2}^2 \beta_{t+h}$	-8.593	-8.806	-6.746	-7.541	-8.582	-7.134
F-stat (P-value)	8.21 (0.00)	5.50 (0.02)	5.37 (0.02)	5.52 (0.02)	8.62 (0.00)	3.69 (0.06)
N	206	206	206	206	206	206

Note: Table shows the results from (1). The dependent variable is daily percent excess returns on the market portfolio. Independent variables include two lags of excess returns on the market portfolio, a five-day window of changes in vaccine progress indicator in years, and dummy variables for each jump date from Baker et al. (2020b) unrelated to news about vaccine progress. The first column is the baseline specification with news applying to all states, deterministic depreciation, base copula correlation of 0.2, probability of success in the application state equal to 0.95 and excludes candidates from China and Russia. Column 2 removes news and depreciation; 3 restricts news to the current state and increases the $\Delta\pi$ from news on positive data releases, positive enrollment and dose starts to 15%, 5% and 5%, respectively; 4 doubles the base copula correlation to 0.4; 5 decreases the probability of success to 0.85 in the application state; and 6 includes candidates from China and Russia. The return on the value-weighted CRSP index is used from January 1, 2020 to October 31, 2020. The table uses Newey-West standard errors with 4 lags; t -statistics are shown in parentheses. Significance levels: * $p < 0.10$, ** $p < 0.05$, *** $p < 0.01$

Table 4: Parameter Values

Parameter	Symbol	Value
Coefficient of relative risk aversion	γ	4.0
Elasticity of intertemporal substitution	ψ	1.5
Rate of time preference	ρ	0.04
Non-pandemic expected output growth	$\mu(0)$	0.055
Non-pandemic output volatility	$\sigma(0)$	0.05

Note: Table shows the preference and non-pandemic parameter values used in estimating the value of a cure.

Table 5: Endogenous Pandemic Parameters via Labor

ℓ^*			Δm_Q				
$K \rightarrow$			$K \rightarrow$				
	0.8471	0.8204	0.7959		0.0517	0.0577	0.0636
$\varepsilon \downarrow$	0.7885	0.7651	0.7435	$\varepsilon \downarrow$	0.0509	0.0565	0.0619
	0.7357	0.7151	0.6960		0.0503	0.0555	0.0605
	0.6880	0.6698	0.6529		0.0497	0.0546	0.0593

Note: Table shows the implied values of equilibrium labor, ℓ^* , and decline in expected growth rate of q in pandemic states, Δm_Q , by fixing the elasticity of expected output with respect to labor $\alpha = 0.5$, exposure to the pandemic unrelated to labor $k = 0.006$, intensity of switching to the pandemic state $\eta = 0.04$, and intensity of switching to the non-pandemic state $\lambda = 0.5$. Each panel varies the exposure to the pandemic via private labor, ε , and via aggregate labor, K . ε increases down the rows and takes the values 0.023, 0.024, 0.025 and 0.026, while K increases left-to-right across columns and takes the values 0.018, 0.024 and 0.030.

Table 6: Externality and Value of a Cure

		ℓ_{cp}^*/ℓ^*			V_{cp}/V		
		K →			K →		
$\varepsilon \downarrow$		0.3762	0.2994	0.2450	0.8661	0.8167	0.7725
		0.3860	0.3083	0.2530	0.8777	0.8309	0.7884
		0.3957	0.3170	0.2609	0.8882	0.8438	0.8031
		0.4049	0.3256	0.2686	0.8975	0.8555	0.8165

Note: The left panel provides a direct measure of the scale of the externality via the ratio of the central planner's solution for optimal labor in the pandemic to that actually chosen by agents. The right panel shows the ratio of the value of a cure as determined by the central planner to that chosen by agents. Both fix the elasticity of expected output with respect to labor $\alpha = 0.5$, exposure to the pandemic unrelated to labor $k = 0.006$, intensity of switching to the pandemic (non-pandemic) state $\eta = 0.4$ ($\lambda = 0.5$). Exposure to the pandemic via private labor, ε , increases down to rows and takes values $\{0.023, 0.024, 0.025, 0.026\}$. Exposure via aggregate labor, K , increases left-to-right and takes values $\{0.018, 0.024, 0.030\}$.

Table 7: Value of a Cure under Parameter Uncertainty

		Low Uncertainty / Low EIS			Low Uncertainty / High EIS			
		$\hat{\lambda}$			$\hat{\lambda}$			
		0.2	0.5	1.0	0.2	0.5	1.0	
$\hat{\eta}$	0.01	0.242	0.114	0.058	0.01	0.242	0.116	0.058
	0.05	0.192	0.102	0.055	0.05	0.185	0.102	0.055
		High Uncertainty / Low EIS			High Uncertainty / High EIS			
		$\hat{\lambda}$			$\hat{\lambda}$			
		0.2	0.5	1.0	0.2	0.5	1.0	
$\hat{\eta}$	0.01	0.633	0.613	0.558	0.01	0.379	0.302	0.222
	0.05	0.456	0.479	0.477	0.05	0.256	0.222	0.186

Note: Table shows the fraction of wealth the agent would be willing to surrender for a one-time transition out of the pandemic state. High (low) EIS sets $\psi = 1.5$ ($\psi = 0.15$). Agents know the parameters λ and η in low uncertainty, and in high uncertainty have posterior standard deviation equal to their point estimates of them. All use coefficient of relative risk aversion $\gamma = 4$, rate of time preference $\rho = 0.04$, elasticity of expected output with respect to labor $\alpha = 0.5$, output volatility $\sigma = 0.05$, expected output growth $\mu = 0.05$, and exposure to the pandemic via private labor $\varepsilon = 0.4$, unrelated to labor $k = 0.1$, and via aggregate labor $K = 0.4$, and P_t intensity $\zeta = 1$.

Table 8: Value of a Permanent Cure

		Low Uncertainty / Low EIS			Low Uncertainty / High EIS			
		$\hat{\lambda}$			$\hat{\lambda}$			
		0.2	0.5	1.0	0.2	0.5	1.0	
$\hat{\eta}$	0.01	0.308	0.136	0.068	0.01	0.327	0.148	0.074
	0.05	0.430	0.214	0.111	0.05	0.429	0.239	0.130
		High Uncertainty / Low EIS			High Uncertainty / High EIS			
		$\hat{\lambda}$			$\hat{\lambda}$			
		0.2	0.5	1.0	0.2	0.5	1.0	
$\hat{\eta}$	0.01	0.813	0.720	0.613	0.01	0.503	0.378	0.265
	0.05	0.831	0.751	0.658	0.05	0.538	0.435	0.335

Note: Table shows the fraction of wealth the agent would exchange to live in a world with no pandemics. High (low) EIS sets $\psi = 1.5$ ($\psi = 0.15$). Agents know the parameters λ and η in low uncertainty, and in high uncertainty have posterior standard deviation equal to their point estimates of them. All use coefficient of relative risk aversion $\gamma = 4$, rate of time preference $\rho = 0.04$, elasticity of expected output with respect to labor $\alpha = 0.5$, output volatility $\sigma = 0.05$, expected output growth $\mu = 0.05$, and exposure to the pandemic via private labor $\varepsilon = 0.4$, unrelated to labor $k = 0.1$, and via aggregate labor $K = 0.4$, and P_t intensity $\zeta = 1$.

Table 9: Value of Information

		Low EIS			High EIS			
		$\hat{\lambda}$			$\hat{\lambda}$			
		0.2	0.5	1.0	0.2	0.5	1.0	
$\hat{\eta}$	0.01	0.733	0.675	0.587	0.01	0.270	0.273	0.209
	0.05	0.708	0.682	0.617	0.05	0.200	0.255	0.236

Note: Table shows the fraction of wealth the agent would be willing to surrender for a one-time transition from high to low parameter uncertainty. High (low) EIS sets $\psi = 1.5$ ($\psi = 0.15$). Agents know the parameters λ and η in low uncertainty, and in high uncertainty have posterior standard deviation equal to their point estimates of them. All use coefficient of relative risk aversion $\gamma = 4$, rate of time preference $\rho = 0.04$, elasticity of expected output with respect to labor $\alpha = 0.5$, output volatility $\sigma = 0.05$, expected output growth $\mu = 0.05$, and exposure to the pandemic via private labor $\varepsilon = 0.4$, unrelated to labor $k = 0.1$, and via aggregate labor $K = 0.4$, and P_t intensity $\zeta = 1$.